Supporting Information

Epimers with distinct mechanical behaviours

Udaya B. Rao Khandavilli,[a] Aoife M. Buckley,[a] Anita R. Maguire,[b] Mangalampalli S. R. N. Kiran,[c] Upadrasta Ramamurty,[d] and Simon E. Lawrence*[a]

[a] *School of Chemistry, Analytical and Biological Chemistry Research Facility, Synthesis and Solid State Pharmaceutical Centre, University College Cork, College Road, Cork, Ireland.*
[b] *School of Chemistry and School of Pharmacy, Analytical and Biological Chemistry Research Facility, Synthesis and Solid State Pharmaceutical Centre, University College Cork, College Road, Cork, Ireland.*
[c] *Department of Physics and Nanotechnology, SRM Institute of Science and Technology, Chennai, 603203, India.*
[d] *School of Mechanical and Aerospace Engineering, Nanyang Technological University, Singapore 639798, Republic of Singapore*

Content	Page number
Synthesis	S2
NMR data	S8
IR data for brittle compounds (**1a-4a)**	S16
IR data for bending compounds (**1b-4b**)	S18
PXRD data for brittle compounds (**1a-4a**)	S20
PXRD data for bending compounds (**1b-4b**)	S22
DSC data for brittle compounds (**1a-4a**)	S24
DSC data for bending compounds (**1b-4b**)	S26
Crystallographic diagrams	S28
Face indexation studies of bending and brittle compounds	S32
Nanoindentation studies for bending and brittle compounds	S38
References	S43

Synthesis of the esters 1-4.

The two diastereomeric series of esters **2'S 1a-4a** and **2'R 1b-4b** were synthesised as summarised in Scheme 1. While the methyl 2-naphthylacetate and ethyl 2-naphthylacetate were prepared by Fischer esterification (96 and 93% respectively), the isopropyl and tert-butyl 2-naphthylacetate were synthesised through an acid chloride intermediate (100% and 85% respectively). With the esters in hand, diazo transfer and the subsequent O–H insertion into (−)-menthol was undertaken.

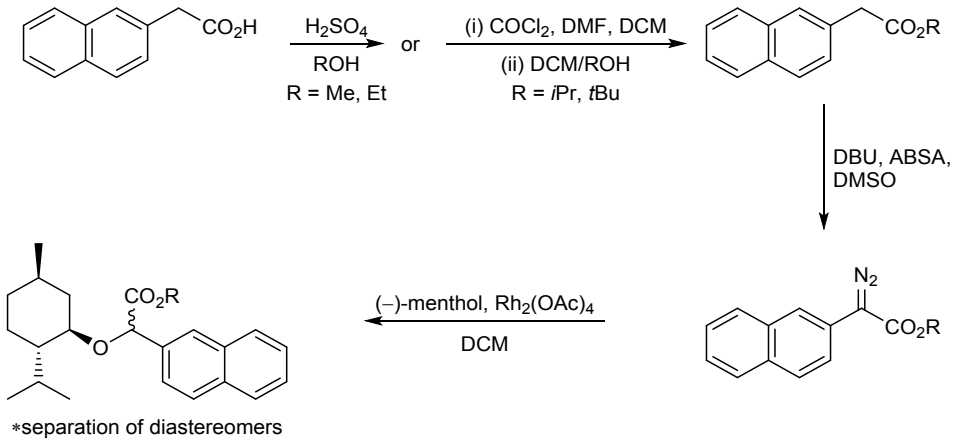

Scheme 1 An overview of the synthesis of the esters.

Transformation of the 2-naphthylacetates to the corresponding 2-naphthyldiazoacetates was achieved through diazo transfer with *p*-ABSA (4-acetamidobenzenesulfonyl azide) and DBU (1,8-Diazabicyclo[5.4.0]undec-7-ene) in DMSO.[1-4] The 2-naphthyldiazoacetates could be prepared on a multi-gram scale (up to ~12 g) and were isolated by column chromatography as orange solids in very good yields (85–92%).

Table 1 *O–H insertion reaction of 2-naphthyldiazoacetates with (−)-menthol.*

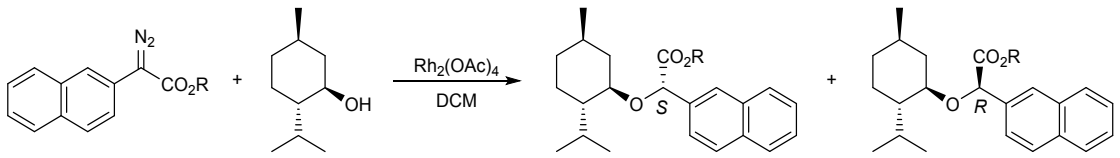

Entry	R	Product	Ratio *2'S* : *2'R*	Yield *2'S* 1a-4a (%)[a]	Yield *2'R* 1b-4b (%)[a]
1	Me	**1**	74:26	29	6
2	Et	**2**	75:25	31	8
3	*i*Pr	**3**	73:27	35	4
4	*t*Bu	**4**	76:24	29	5

[a] Yields of pure epimers recovered following column chromatography and recrystallization from acetonitrile.

The O–H insertion reactions were carried out by adding rhodium acetate (1 mol%) to a stirring solution of naphthyldiazoacetate and (−)-menthol in DCM. Reactions were complete after 2 hours at room temperature and following evaporation under reduced

pressure, a ^{1}H NMR spectrum of the crude reaction mixture was obtained in each case. For compounds **1-4** the epimeric ratio of the 2′*S*:2′*R* isomers was determined by integration of characteristic signals in the ^{1}H NMR spectra – very similar ratios were seen across the series ~3:1 2′*S*:2′*R* (**Table 1**). The reactions were generally efficient with little evidence for competing carbenoid processes in the ^{1}H NMR spectra of the crude reaction mixtures.

Column chromatography was performed on the crude reaction mixtures to isolate the individual epimers with the 2′S consistently eluting as the less polar epimer. Across the series, recrystallization from acetonitrile, following chromatographic separation, was employed as a means of obtaining analytically pure samples of each of the epimers **1a-4a** and **1b-4b**. Isolated yields of pure epimers following recrystallization were moderate (29–35%) for the 2′*R* isomers and very poor (4–8%) for the 2′*S* isomers.

Each of the esters synthesised by O–H insertion were novel compounds and were fully characterised during this work. Characteristic ^{1}H and ^{13}C NMR signals are outlined below.

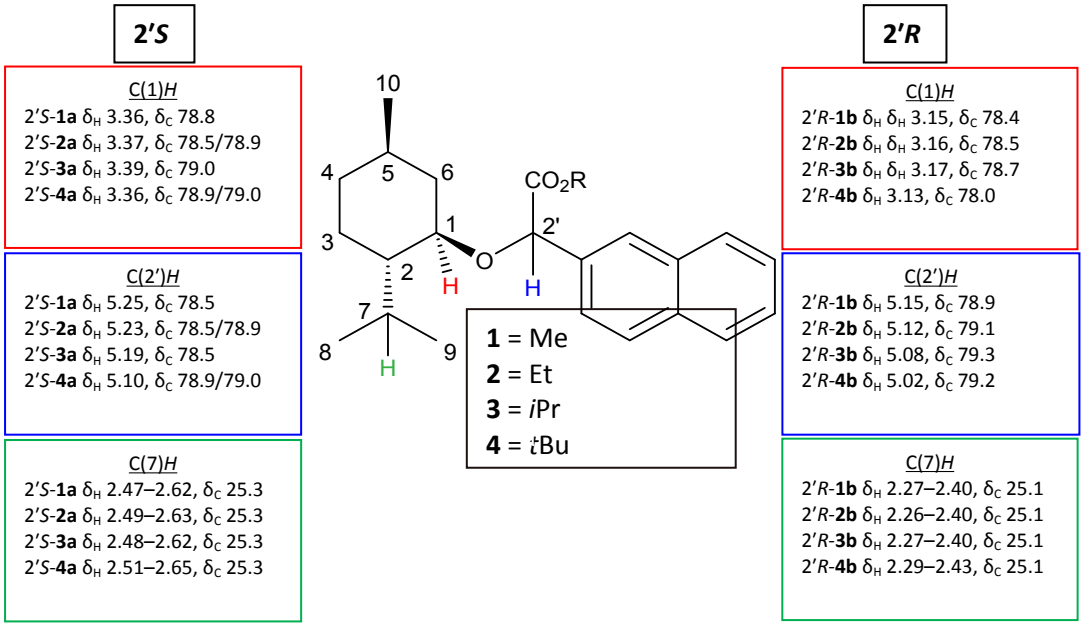

Methyl (2′*S*)-(1*R*,2*R*,5*S*)-menthyloxy-2′-naphthylacetate, (2′*S*)-1a

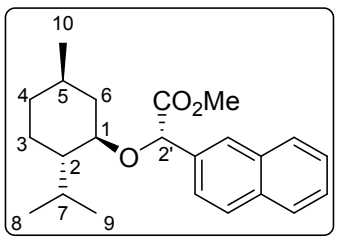

Less polar, major isomer, white solid (2′*S*)-**1a** (0.69 g, 29%), mp 87–89 °C; (Found C, 78.06; H, 8.53. $C_{23}H_{30}O_3$ requires C, 77.93; H, 8.53%); $[\alpha]_D^{20}$ = −14.2 (*c* 1.0, $CHCl_3$); ν_{max}/cm^{-1} (neat) 2929, 1747 (C=O), 1430, 1100, 751, 480; ^{1}H NMR (400 MHz): δ 0.66–1.15 [12H, m, contains, 3H, m, one each of C(6)H_2, C(4)H_2, C(3)H_2, 2 x overlapping 3H, d, *J* ~7.0, one of C(8)H_3 or C(9)H_3 and C(10)H_3 at 0.87, 3H, d, *J* 7.0, one of C(8)H_3 or C(9)H_3 at 0.97], 1.24–1.47 [2H, m, C(5)*H*, C(2)*H*], 1.58–1.73 [2H, m, one each of C(4)H_2 and C(3)H_2], 2.06 [1H, bd, *J* 11.8, one of C(6)H_2], 2.47–2.62 [1H, m, C(7)*H*], 3.36 [1H, td, *J* 10.5, 4.1, C(1)*H*], 3.69 (3H, s, CO_2CH_3), 5.25 (1H, s, C(2′)*H*), 7.42-7.51 (2H, m, aromatic *H*), 7.60 (1H, dd, *J* 8.5, 1.2, aromatic *H*), 7.78–7.88 (3H, m, aromatic *H*), 7.92 (1H, bs, aromatic *H*); ^{13}C NMR (100.6

MHz): δ 16.1 [CH_3, C(8)H_3 or C(9)H_3], 21.3 [CH_3, C(8)H_3 or C(9)H_3], 22.3 [CH_3, C(10)H_3], 23.1 [CH_2, one of C(4)H_2 or C(3)H_2], 25.3 [CH, C(7)H], 31.5 [CH, C(5)H], 34.4 [CH_2, one of C(4)H_2 or C(3)H_2], 40.4 [CH_2, C(6)H_2], 48.5 [CH, C(2)H], 52.2 (CH_3, CO_2CH_3), 78.5 [CH, C(2′)H], 78.8 [CH, C(1)H], 124.7 (CH, aromatic CH), 126.19, (CH, aromatic CH), 126.22 (CH, aromatic CH), 126.3 (CH, aromatic CH) 127.7 (CH, aromatic CH), 128.2 (CH, aromatic CH), 128.3 (CH, aromatic CH), 133.2 (C, aromatic C), 133.4 (C, aromatic C), 135.2 (C, aromatic C), 172.0 (C, CO).

Methyl (2′*R*)-(1*R*,2*R*,5*S*)-menthyloxy-2′-naphthylacetate, (2′*R*)-1b

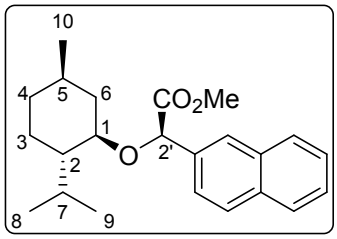

More polar, minor isomer, white solid, (2′*R*)-**1b** (0.15, 6%), mp 125–127 °C; $[\alpha]_D^{20}$ = −185.9 (*c* 1.0, $CHCl_3$); ν_{max}/cm^{-1} (neat) 2930, 1750 (C=O), 1160, 1097, 816, 757, 479; ^{1}H NMR (400 MHz): δ 0.42 [3H, d, *J* 6.9, C(8)H_3 or C(9)H_3], 0.78–0.99 [8H, m, contains, 2H, m, one each of C(4)H_2, C(3)H_2, 3H, d, *J* 7.1, C(8)H_3 or C(9)H_3 at 0.86 and 3H, d, J 6.5, C(10)H_3 at 0.93], 1.04 [1H, q, *J* 11.1, one of C(6)H_2], 1.21–1.34 [1H, m, C(5)*H*], 1.36–1.47 [1H, m, C(2)*H*], 1.52–1.67 [2H, m, one each of C(4)H_2 and C(3)H_2], 2.16 [1H, bd, *J* 11.8, one of C(6)H_2], 2.27–2.40 [1H, m, C(7)*H*], 3.15 [1H, td, *J* 10.5, 4.1, C(1)*H*], 3.70 (3H, s, CO_2CH_3), 5.15 (1H, s, C(2′)*H*), 7.45–7.51 (2H, m, aromatic *H*), 7.58 (1H, dd, J 8.5, 1.3, aromatic *H*), 7.79–7.89 (3H, m, aromatic *H*), 7.90 (1H, bs, aromatic *H*); ^{13}C NMR (100.6 MHz): δ 15.6 [CH_3, C(8)H_3 or C(9)H_3], 21.1 [CH_3, C(8)H_3 or C(9)H_3], 22.3 [CH_3, C(10)H_3], 22.9 [CH_2, one of C(4)H_2 or C(3)H_2], 25.1 [CH, C(7)H], 31.6 [CH, C(5)H], 34.4 [CH_2, one of C(4)H_2 or C(3)H_2], 40.2 [CH_2, C(6)H_2], 48.1 [CH, C(2)H], 52.3 (CH_3, CO_2CH_3), 78.4 [CH, C(1)H], 78.9 [CH, C(2′)], 125.0 (CH, aromatic CH), 126.27 (CH, aromatic CH), 126.32 (CH, aromatic CH), 127.0 (CH, aromatic CH), 127.7 (CH, aromatic CH), 128.1 (CH, aromatic CH), 128.4 (CH, aromatic CH), 133.1 (C, aromatic C), 133.4 (C, aromatic C), 134.5 (C, aromatic C), 172.1 (C, CO).

Ethyl (2′*S*)-(1*R*,2*R*,5*S*)-menthyloxy-2′-naphthylacetate, (2′*S*)-2a

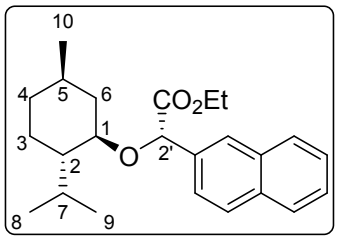

Less polar, major isomer, white solid, (2′*S*)-**2a** (2.11 g, 31%), mp 92–94 °C; (Found C, 78.39; H, 8.84. $C_{24}H_{32}O_3$ requires C, 78.22; H, 8.75%); $[\alpha]_D^{20}$ = −23.0 (*c* 1.0, $CHCl_3$); ν_{max}/cm^{-1} (neat) 1743 (C=O), 1184, 1100, 817, 751, 479; ^{1}H NMR (400 MHz): δ 0.78–1.08 [12H, m, contains, 3H, m, one each of C(6)H_2, C(4)H_2, C(3)H_2, 2 x overlapping 3H, d, *J* ~7.0 one of C(8)H_3 or C(9)H_3 and C(10)H_3 at 0.87, 3H, d, *J* 7.1, one of C(8)H_3 or C(9)H_3 at 0.97], 1.20 (3H, t, *J* 7.1, $CO_2CH_2CH_3$), 1.25–1.45 [2H, m, C(5)*H*, C(2)*H*], 1.59–1.71 [2H, m, one each of C(4)H_2 and C(3)H_2], 2.07 [1H, bd, *J* 11.6, one of C(6)H_2], 2.49–2.63 [1H, m, C(7)*H*], 3.37 [1H, td, *J* 10.5, 4.2, C(1)*H*], 4.08–4.24 (2H, m, $CO_2CH_2CH_3$), 5.23 (1H, s, C(2′)*H*), 7.42–7.50 (2H, m, aromatic *H*), 7.61 (1H, dd, *J* 8.5, 1.4, aromatic *H*), 7.77–7.88 (3H, m, aromatic *H*), 7.93 (1H, bs, aromatic *H*); ^{13}C NMR (100.6 MHz): δ 14.1, (CH_3, $CO_2CH_2CH_3$), 16.2 [CH_3, C(8)H_3 or C(9)H_3], 21.3 [CH_3, C(8)H_3 or C(9)H_3], 22.3 [CH_3, C(10)H_3], 23.2 [CH_2, one of C(4)H_2 or C(3)H_2], 25.3 [CH, C(7)H], 31.6 [CH, C(5)H], 34.5 [CH_2, one of C(4)H_2 or C(3)H_2], 40.5 [CH_2, C(6)H_2], 48.5 [CH, C(2)H], 61.1 (CH_2, $CO_2CH_2CH_3$), 78.5 [CH, C(1)H or C(2′)H], 78.9 [CH, C(1)H or C(2′)H], 124.8 (CH, aromatic CH), 126.13, (CH, aromatic CH), 126.16

(CH, aromatic *C*H), 126.2 (CH, aromatic *C*H) 127.7 (CH, aromatic *C*H), 128.20 (CH, aromatic *C*H), 128.24 (CH, aromatic *C*H), 133.2 (C, aromatic *C*), 133.3 (C, aromatic *C*), 135.4 (C, aromatic *C*), 171.6 (C, *C*O).

Ethyl (2′*R*)-(1*R*, 2*R*, 5*S*)-menthyloxy-2′-naphthylacetate, (2′*R*)-2b

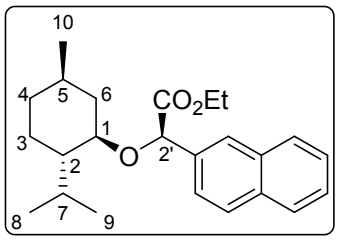

More polar, minor isomer, white solid, (2′*R*)-**2b** (0.55, 8%), mp 79–80 °C; (Found C, 78.35; H, 8.90. $C_{24}H_{32}O_3$ requires C, 78.22; H, 8.75%); $[\alpha]_D^{20} = -163.3$ (*c* 1.0, $CHCl_3$); ν_{max}/cm^{-1} (neat) 2954, 1742 (C=O), 1179, 1166, 1089, 817, 755, 479; ^{1}H NMR (400 MHz): δ 0.45 [3H, d, *J* 6.9, C(8)H_3 or C(9)H_3], 0.80–0.96 [8H, m, contains, 2H, m, one each of C(4)H_2, C(3)H_2, 3H, d, *J* 7.0, C(8)H_3 or C(9)H_3 at 0.86 and 3H, d, *J* 6.5, C(10)H_3 at 0.93], 1.06 [1H, q, *J* 11.2, C(6)*H*], 1.20 (3H, t, *J* 7.0, $CO_2CH_2CH_3$), 1.24–1.48 [2H, m, C(5)*H* and C(2)*H*], 1.54–1.68 [2H, m, one each of C(4)H_2 and C(3)H_2], 2.16 [1H, bd, *J* 12.0, one of C(6)H_2], 2.26–2.40 [1H, m, C(7)*H*], 3.16 [1H, td, *J* 10.5, 4.1, C(1)*H*], 4.08–4.26 (2H, m, $CO_2CH_2CH_3$), 5.12 (1H, s, C(2′)*H*), 7.45–7.52 (2H, m, aromatic *H*), 7.59 (1H, dd, J 8.5, 1.4, aromatic *H*), 7.80–7.88 (3H, m, aromatic *H*), 7.91 (1H, bs, aromatic *H*); ^{13}C NMR (100.6 MHz): δ 14.1 (CH_3, $CO_2CH_2CH_3$), 15.7 [CH_3, *C*(8)H_3 or *C*(9)H_3], 21.1 [CH_3, *C*(8)H_3 or *C*(9)H_3], 22.4 [CH_3, *C*(10)H_3], 22.9 [CH_2, one of *C*(4)H_2 or *C*(3)H_2], 25.1 [CH, *C*(7)H], 31.6 [CH, *C*(5)H], 34.4 [CH_2, one of *C*(4)H_2 or *C*(3)H_2], 40.4 [CH_2, *C*(6)H_2], 48.1 [CH, *C*(2)H], 61.2 (CH_2, $CO_2CH_2CH_3$), 78.5 [CH, *C*(1)H], 79.1 [CH, *C*(2′)], 125.0 (CH, aromatic *C*H), 126.2 (CH, aromatic *C*H), 126.3 (CH, aromatic *C*H), 126.9 (CH, aromatic *C*H), 127.7 (CH, aromatic *C*H), 128.1 (CH, aromatic *C*H), 128.3 (CH, aromatic *C*H), 133.1 (C, aromatic *C*), 133.4 (C, aromatic *C*), 134.7 (C, aromatic *C*), 171.7 (C, *C*O).

Isopropyl (2′*S*)-(1*R*, 2*R*, 5*S*)-menthyloxy-2′-naphthylacetate, (2′*S*)-3a

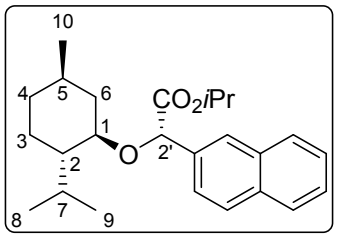

Less polar, major isomer, white solid, (2′*S*)-**3a** (2.43 g, 35%), mp 55–56 °C; (Found C, 78.66; H, 8.90. $C_{25}H_{34}O_3$ requires C, 78.49; H, 8.96%); $[\alpha]_D^{20} = -29.6$ (*c* 1.0, $CHCl_3$); ν_{max}/cm^{-1} (neat) 1737 (C=O), 1191, 1099, 817, 815, 755, 476; ^{1}H NMR (400 MHz): δ 0.78–1.08 [12H, m, contains, 3H, m, one each of C(6)H_2, C(4)H_2, C(3)H_2, 2 x overlapping 3H, d, *J* ~7.0 one of C(8)H_3 or C(9)H_3 and C(10)H_3 at 0.87 and 0.88, 3H, d, *J* 7.0, one of C(8)H_3 or C(9)H_3 at 0.96], 1.13 [3H, d, *J* 6.2, one of $CO_2CH(CH_3)_2$], 1.22 [3H, d, *J* 6.3, one of $CO_2CH(CH_3)_2$], 1.26–1.46 [2H, m, C(5)*H*, C(2)*H*], 1.60–1.72 [2H, m, one each of C(4)H_2 and C(3)H_2], 2.07 [1H, bd, *J* 12.0, one of C(6)H_2], 2.48–2.62 [1H, m, C(7)*H*], 3.39 [1H, td, *J* 10.5, 4.1, C(1)*H*], 5.02 (1H, septet, *J* 6.3, $CO_2CH(CH_3)_2$], 5.19 (1H, s, C(2′)*H*), 7.42–7.51 (2H, m, aromatic *H*), 7.61 (1H, dd, *J* 8.5, 1.4, aromatic *H*), 7.78–7.88 (3H, m, aromatic *H*), 7.93 (1H, bs, aromatic *H*); ^{13}C NMR (100.6 MHz): δ 16.3 [CH_3, *C*(8)H_3 or *C*(9)H_3], 21.2 [CH_3, *C*(8)H_3 or *C*(9)H_3], 21.5 [CH_3, one of $CO_2CH(CH_3)_2$], 21.8 [CH_3, one of $CO_2CH(CH_3)_2$], 22.3 [CH_3, *C*(10)H_3], 23.2 [CH_2, one of *C*(4)H_2 or *C*(3)H_2], 25.3 [CH, *C*(7)H], 31.5 [CH, *C*(5)H], 34.4 [CH_2, one of *C*(4)H_2 or *C*(3)H_2], 40.5 [CH_2, *C*(6)H_2], 48.4 [CH, *C*(2)H], 68.7 [CH, $CO_2CH(CH_3)_2$], 78.5 [CH, *C*(2′)H], 79.0 [CH, *C*(1)H], 124.7 (CH, aromatic *C*H), 126.0, (CH, aromatic *C*H), 126.07 (CH, aromatic *C*H), 126.12 (CH, aromatic *C*H) 127.7 (CH, aromatic *C*H), 128.1 (CH,

aromatic *C*H), 128.2 (CH, aromatic *C*H), 133.2 (C, aromatic *C*), 133.3 (C, aromatic *C*), 135.5 (C, aromatic *C*), 171.1 (C, *C*O).

Isopropyl (2′*R*)-(1*R*,2*R*,5*S*)-menthyloxy-2′-naphthylacetate, (2′*R*)-3b

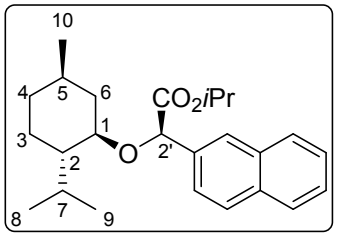

More polar, minor isomer, white solid, (2′*R*)-**3b** (0.26 g, 4%), mp 90–92 °C; (Found C, 78.42; H, 8.87. $C_{25}H_{34}O_3$ requires C, 78.49; H, 8.96%); $[\alpha]_D^{20} = -147.0$ (*c* 1.0, $CHCl_3$); ν_{max}/cm^{-1} (neat) 1730 (C=O), 1181, 1084, 812, 761, 480; ^{1}H NMR (400 MHz): δ 0.48 [3H, d, *J* 6.9, C(8)H_3 or C(9)H_3], 0.78–0.98 [8H, m, contains, 2H, m, one each of C(4)H_2, C(3)H_2, 3H, d, *J* 6.9, C(8)H_3 or C(9)H_3 at 0.86 and 3H, d, *J* 6.4, C(10)H_3 at 0.93], 1.01–1.13 [4H, m, contains 1H, m, one of C(6)H_2 and 3H, d, *J* 6.3, one of $CO_2CH(CH_3)_2$ at 1.09], 1.19–1.37 [4H, m, contains 3H, d, *J* 6.2, one of $CO_2CH(CH_3)_2$ at 1.23 and 1H, m C(5)*H*], 1.37–1.48 [1H, m, C(2)*H*], 1.53-1.70 [2H, m, one each of C(4)H_2 and C(3)H_2], 2.16 [1H, bd, *J* 11.8, one of C(6)H_2], 2.27–2.40 [1H, m, C(7)*H*], 3.17 [1H, td, *J* 10.5, 4.0, C(1)*H*], 5.04 [1H, septet, *J* 6.2, $CO_2CH(CH_3)_2$], 5.08 [1H, s, C(2′)*H*], 7.44–7.52 (2H, m, aromatic *H*), 7.58 (1H, finely split d, *J* 8.5, ~1.5, aromatic *H*), 7.79–7.89 (3H, m, aromatic *H*), 7.90 (1H, bs, aromatic *H*) ; ^{13}C NMR (100.6 MHz): δ 15.7 [CH_3, *C*(8)H_3 or *C*(9)H_3], 21.1 [CH_3, *C*(8)H_3 or *C*(9)H_3], 21.5 [CH_3, one of $CO_2CH(CH_3)_2$], 21.7 [CH_3, one of $CO_2CH(CH_3)_2$], 22.3 [CH_3, *C*(10)H_3], 22.9 [CH_2, one of *C*(4)H_2 or *C*(3)H_2], 25.1 [CH, *C*(7)H], 31.6 [CH, *C*(5)H], 34.4 [CH_2, one of *C*(4)H_2 or *C*(3)H_2], 40.5 [CH_2, *C*(6)H_2], 48.1 [CH, *C*(2)H], 68.6 [CH, $CO_2CH(CH_3)_2$], 78.7 [CH, *C*(1)H], 79.3 [CH, *C*(2′)], 125.0 (CH, aromatic *C*H), 126.1 (CH, aromatic *C*H), 126.2 aromatic *C*H), 128.2 (CH, aromatic *C*H), 133.1 (C, aromatic *C*), 133.3 (C, aromatic *C*), 134.8 (C, aromatic *C*), 171.3 (C, *C*O).

***tert*-Butyl (2′*S*)-(1*R*,2*R*,5*S*)-menthyloxy-2′-naphth-2-ylacetate, (2′*S*)-4a**

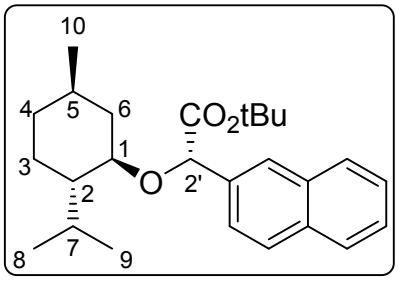

Less polar, minor isomer, white solid, (2′*S*)-**4a** (2.35, 29%), mp 77–79 °C; (Found C, 78.75; H, 9.08. $C_{26}H_{36}O_3$ requires C, 78.75; H, 9.15%); $[\alpha]_D^{20} = -33.1$ (*c* 1.0, $CHCl_3$); ν_{max}/cm^{-1} (neat) 2953, 1737 (C=O), 1147, 1095, 760; ^{1}H NMR (400 MHz): δ 0.78–1.08 [12H, m, contains, 3H, m, one each of C(6)H_2, C(4)H_2, C(3)H_2, 2 x overlapping 3H, d, *J* ~7.0, C(8)H_3 or C(9)H_3 and C(10)H_3 at 0.87 and 0.88 and 3H, d, *J* 7.1, C(8)H_3 or C(9)H_3 at 0.96], 1.26–1.46 [11H, m, contains 2H, m, C(5)*H*, C(2)*H* and 9H, s, $C(CH_3)_3$ at 1.36], 1.60–1.72 [2H, m, one each of C(4)H_2 and C(3)H_2], 2.08 [1H, bd, *J* 11.6, one of C(6)H_2], 2.51–2.65 [1H, m, C(7)*H*], 3.36 [1H, td, *J* 10.5, 4.1, C(1)*H*], 5.10 [1H, s, C(2′)*H*], 7.42–7.51 (2H, m, aromatic *H*), 7.60 (1H, dd, J 8.5, 1.4, aromatic *H*), 7.77–7.89 (3H, m, aromatic *H*), 7.92 (1H, s, aromatic *H*); ^{13}C NMR (100.6 MHz): δ 16.4 [CH_3, *C*(8)H_3 or *C*(9)H_3], 21.3 [CH_3, *C*(8)H_3 or *C*(9)H_3], 22.4 [CH_3, *C*(10)H_3], 23.2 [CH_2, one of *C*(4)H_2 or *C*(3)H_2], 25.3 [CH, *C*(7)H], 28.0 [CH_3, $CO_2C(CH_3)_3$], 31.6 [CH, *C*(6)H], 34.5 [CH_2, one of *C*(4)H_2 or *C*(3)H_2], 40.5 [CH_2, *C*(6)H_2], 48.4 [CH, *C*(2)H], 78.9 [CH, *C*(1)H or *C*(2′)H], 79.0 [CH, *C*(1)H or *C*(2′)H], 81.6 [C, $CO_2C(CH_3)_3$], 124.8 (CH, aromatic *C*H), 125.99, (CH, aromatic *C*H), 126.06 (CH, aromatic *C*H), 126.1 (CH, aromatic *C*H) 127.7 (CH, aromatic

*C*H), 128.0 (CH, aromatic *C*H), 128.2 (CH, aromatic *C*H), 133.21 (C, aromatic *C*), 133.23 (C, aromatic *C*), 135.8 (C, aromatic *C*), 170.8 (C, *C*O).

***tert*-Butyl (2′*R*)-(1*R*,2*R*,5*S*)-menthyloxy-2′-naphth-2-ylacetate, (2′*R*)-4b**

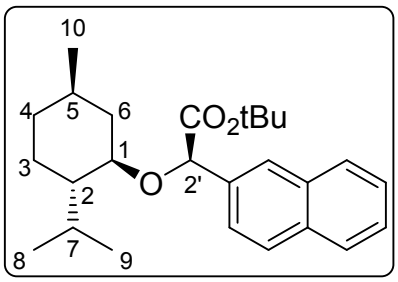

More polar, minor isomer, white solid, (2′*R*)-**4b** (0.52, 5%), mp 92–93 °C; (Found C, 78.64; H, 9.06. $C_{26}H_{36}O_3$ requires C, 78.75; H, 9.15%); $[\alpha]_D^{20}$ = −156.1 (*c* 1.0, $CHCl_3$); ν_{max}/cm^{-1} (neat) 2920, 1732 (C=O), 1148, 1084, 817; ^{1}H NMR (400 MHz): δ 0.46 [3H, d, *J* 6.9, C(8)H_3 or C(9)H_3], 0.75–0.99 [8H, m, contains, 2H, m, one each of C(4)H_2, C(3)H_2, 3H, d, *J* 7.1, C(8)H_3 or C(9)H_3 at 0.86 and 3H, d, *J* 6.5, C(10)H_3 at 0.93], 1.05 [1H, q, *J* 11.1, one of C(6)H_2], 1.21–1.49 [11H, m, contains 2H, m, C(5)*H* and C(2)*H*, and 9H, s, C(CH_3)$_3$ at 1.37], 1.54–1.67 [2H, m, one each of C(4)H_2 and C(3)H_2], 2.18 [1H, bd, *J* 11.7, one of C(6)H_2], 2.29–2.43 [1H, m, C(7)*H*], 3.13 [1H, td, *J* 10.5, 4.1, C(1)*H*], 5.02 [1H, s, C(2′)*H*], 7.43–7.53 (2H, m, aromatic *H*), 7.57 (1H, dd, *J* 8.5, 1.4, aromatic *H*), 7.78–7.93 (3H, m, aromatic *H*), 7.89 (1H, s, aromatic *H*); ^{13}C NMR (100.6 MHz): δ 15.7 [CH_3, *C*(8)H_3 or *C*(9)H_3], 21.1 [CH_3, *C*(8)H_3 or *C*(9)H_3], 22.4 [CH_3, *C*(10)H_3], 22.9 [CH_2, one of *C*(4)H_2 or *C*(3)H_2], 25.1 [CH, *C*(7)H], 27.9 [CH_3, $CO_2C(CH_3)_3$], 31.6 [CH, *C*(5)H], 34.4 [CH_2, one of *C*(4)H_2 or *C*(3)H_2], 40.4 [CH_2, *C*(6)H_2], 48.1 [CH, *C*(2)H], 78.0 [CH, *C*(1)H], 79.2 [CH, *C*(2′)], 81.5 [C, $CO_2C(CH_3)_3$], 125.1 (CH, aromatic *C*H), 126.07 (CH, aromatic *C*H), 126.10 (CH, aromatic *C*H), 126.8 (CH, aromatic *C*H), 127.8 (CH, aromatic *C*H), 128.13 (CH, aromatic *C*H), 128.15 (CH, aromatic *C*H), 133.1 (C, aromatic *C*), 133.3 (C, aromatic *C*), 135.1 (C, aromatic *C*), 170.9 (C, *C*O).

NMR data

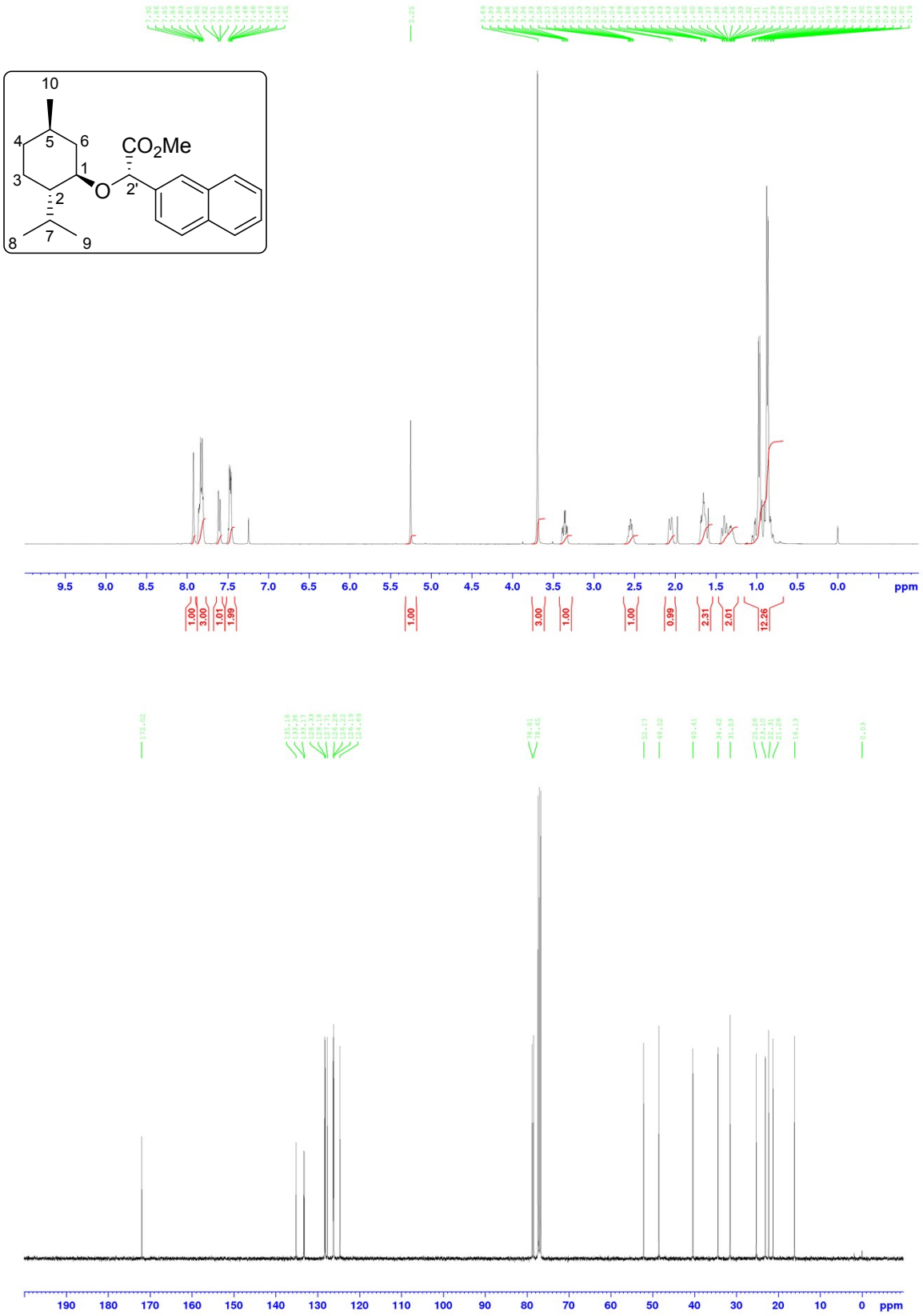

Figure 1. ^{1}H and ^{13}C NMR data for (2′*S*)-Me, **1a**

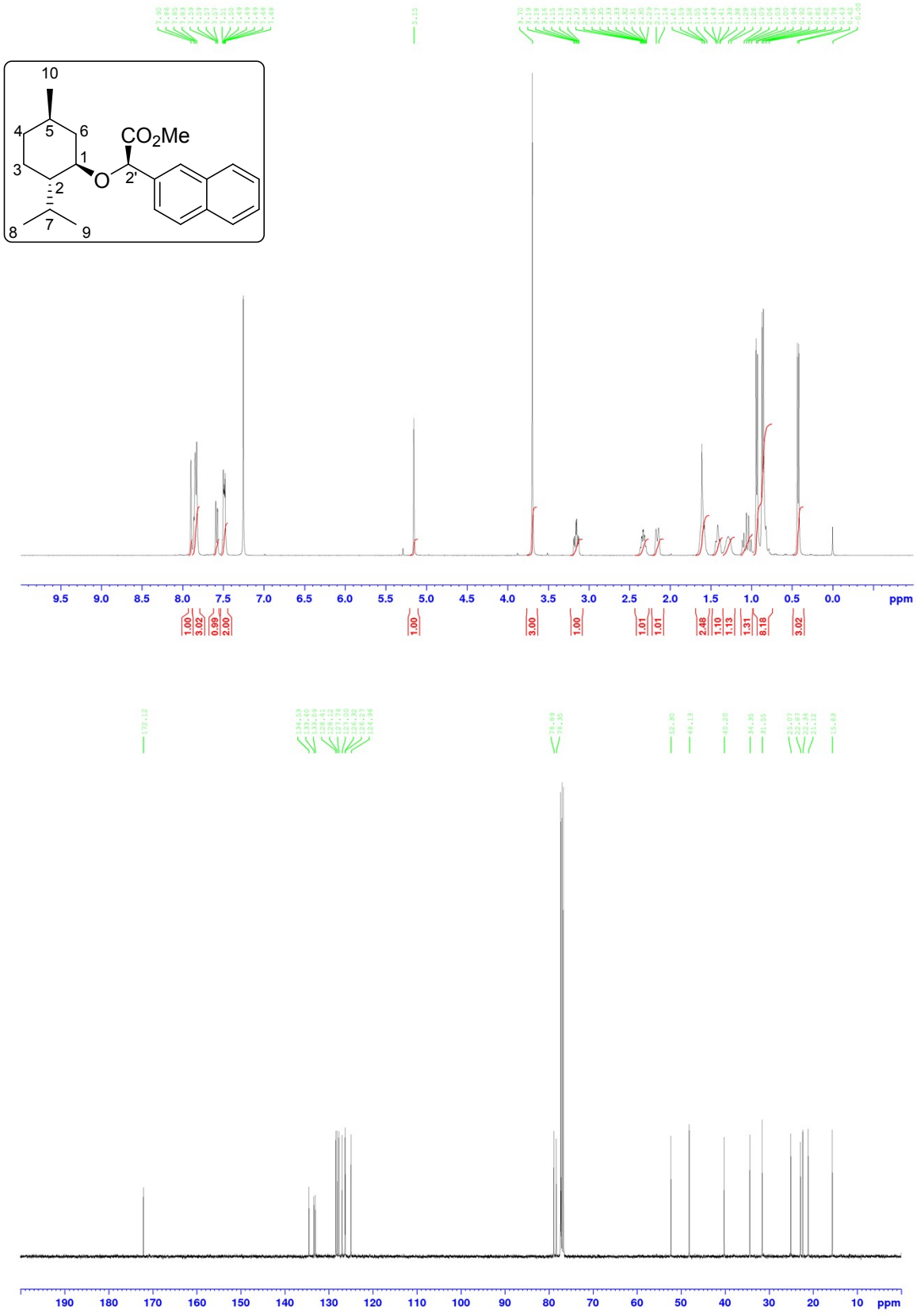

Figure 2. ^{1}H and ^{13}C NMR data for (2′*R*)-Me, **1b**

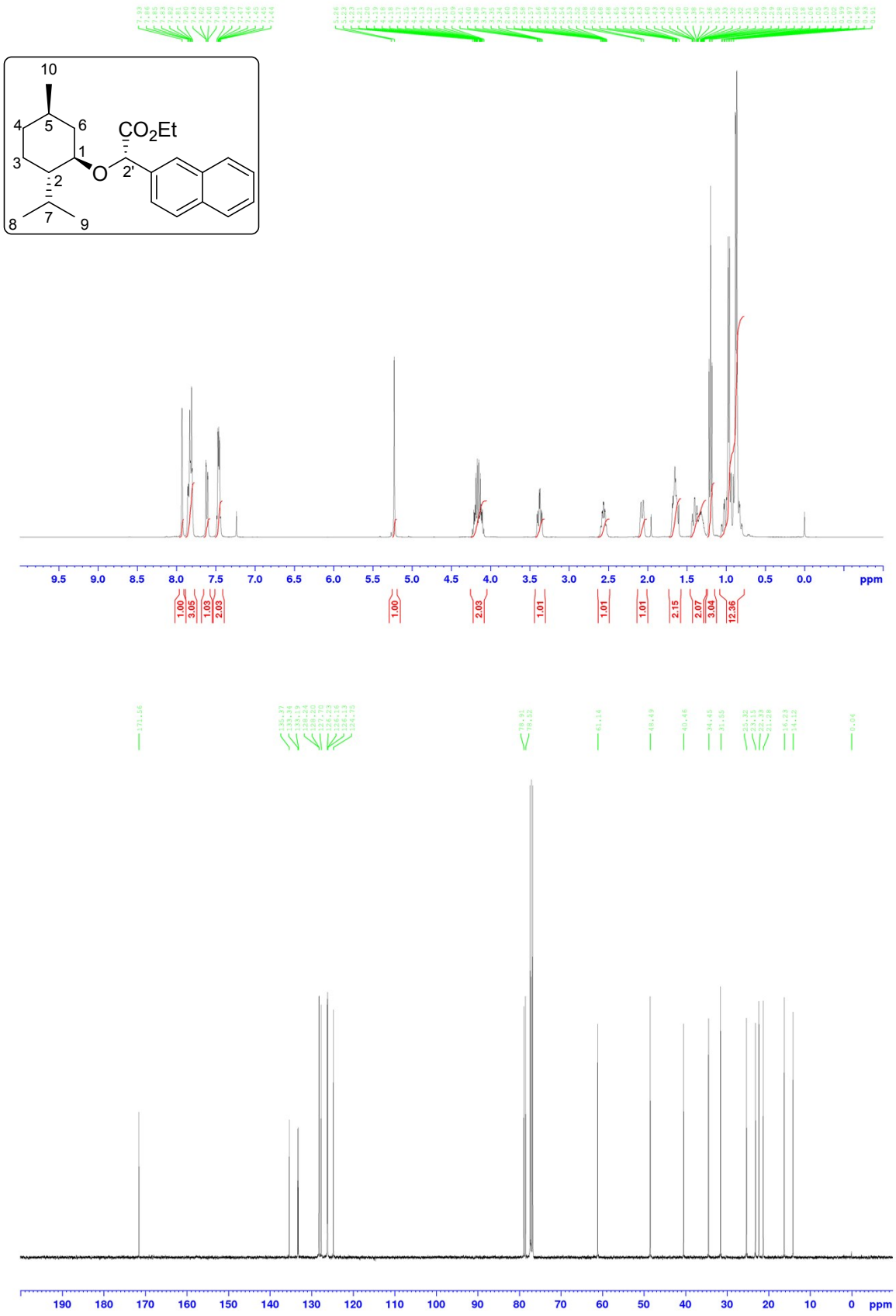

Figure 3. ^{1}H and ^{13}C NMR data for (2′*S*)-Et, **2a**

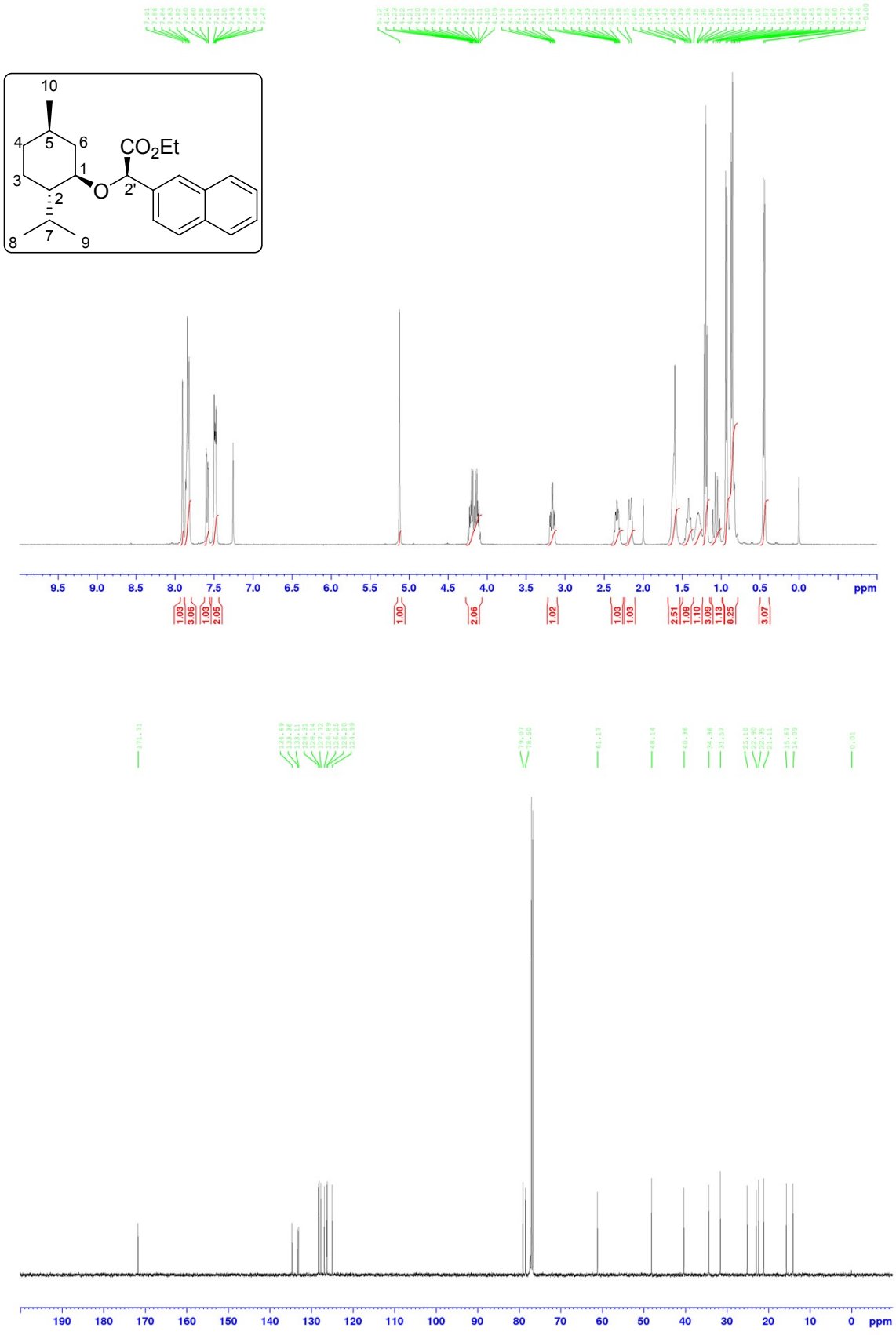

Figure 4. ^{1}H and ^{13}C NMR data for (2′*R*)-Et, **2b**

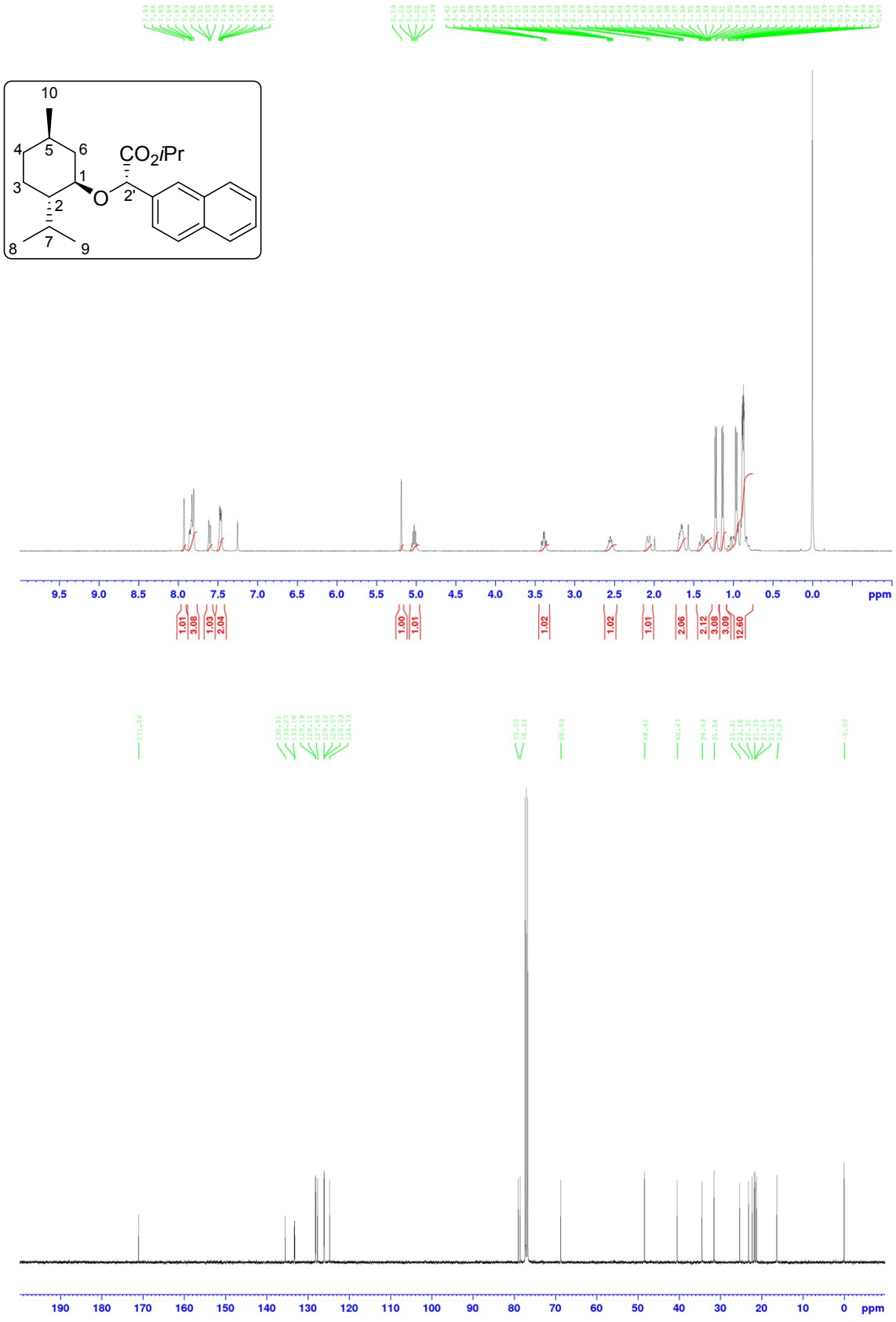

Figure 5. ^{1}H and ^{13}C NMR data for (2′*S*)-*i*Pr, **3a**

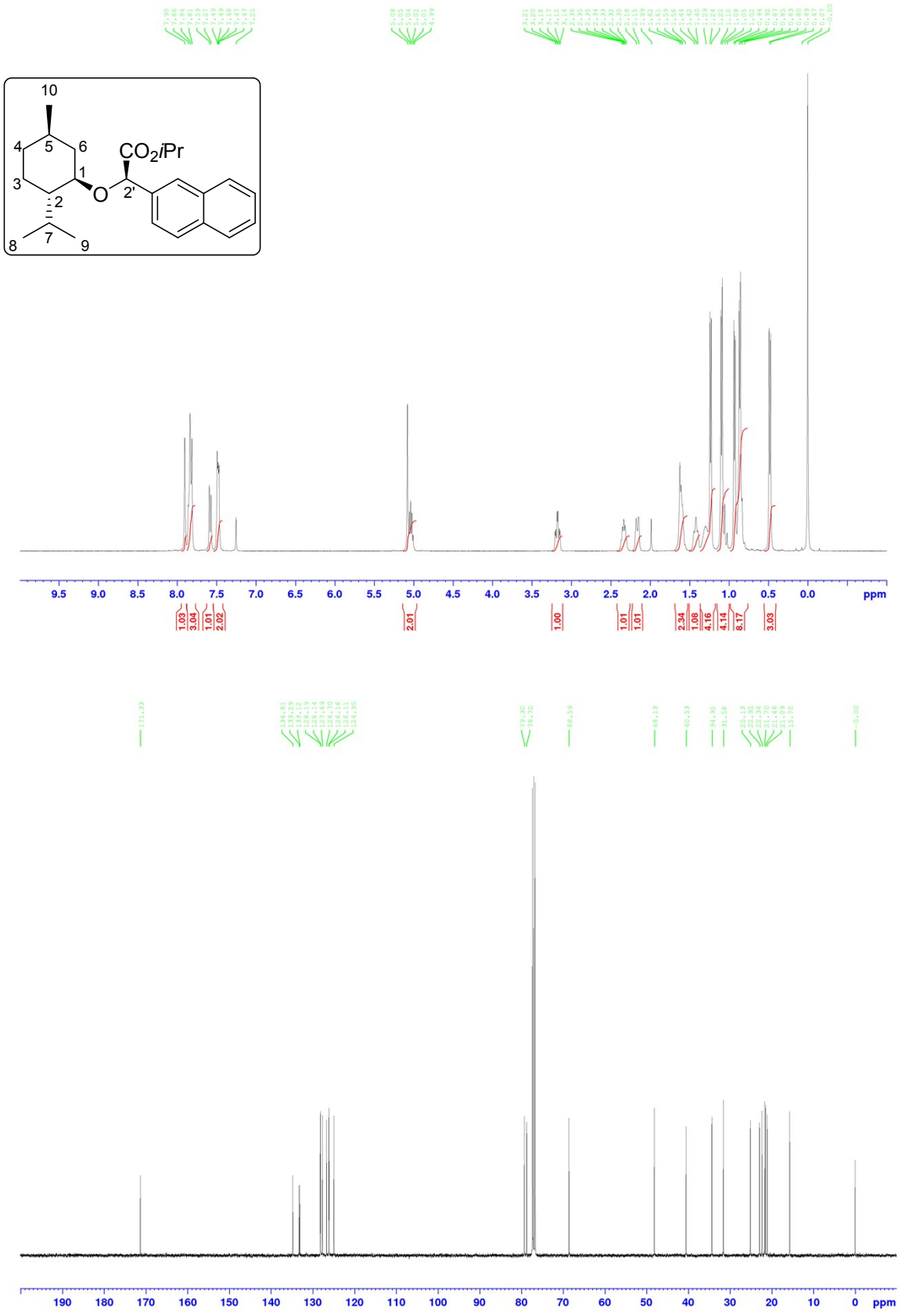

Figure 6. ^{1}H and ^{13}C NMR data for (2′*R*)-*i*Pr, **3b**

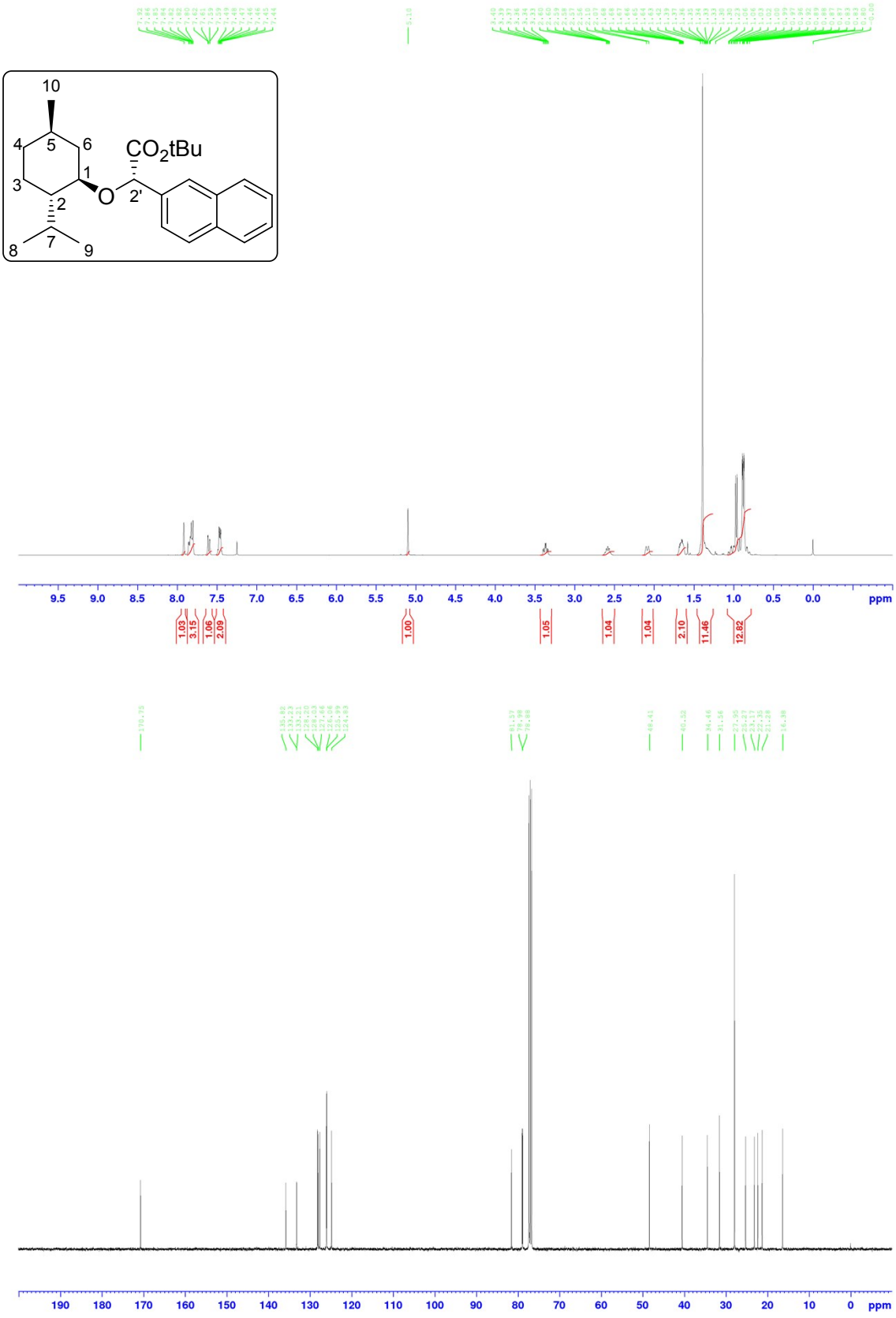

Figure 7. ^{1}H and ^{13}C NMR data for (2′*S*)-*t*Bu, **4a**

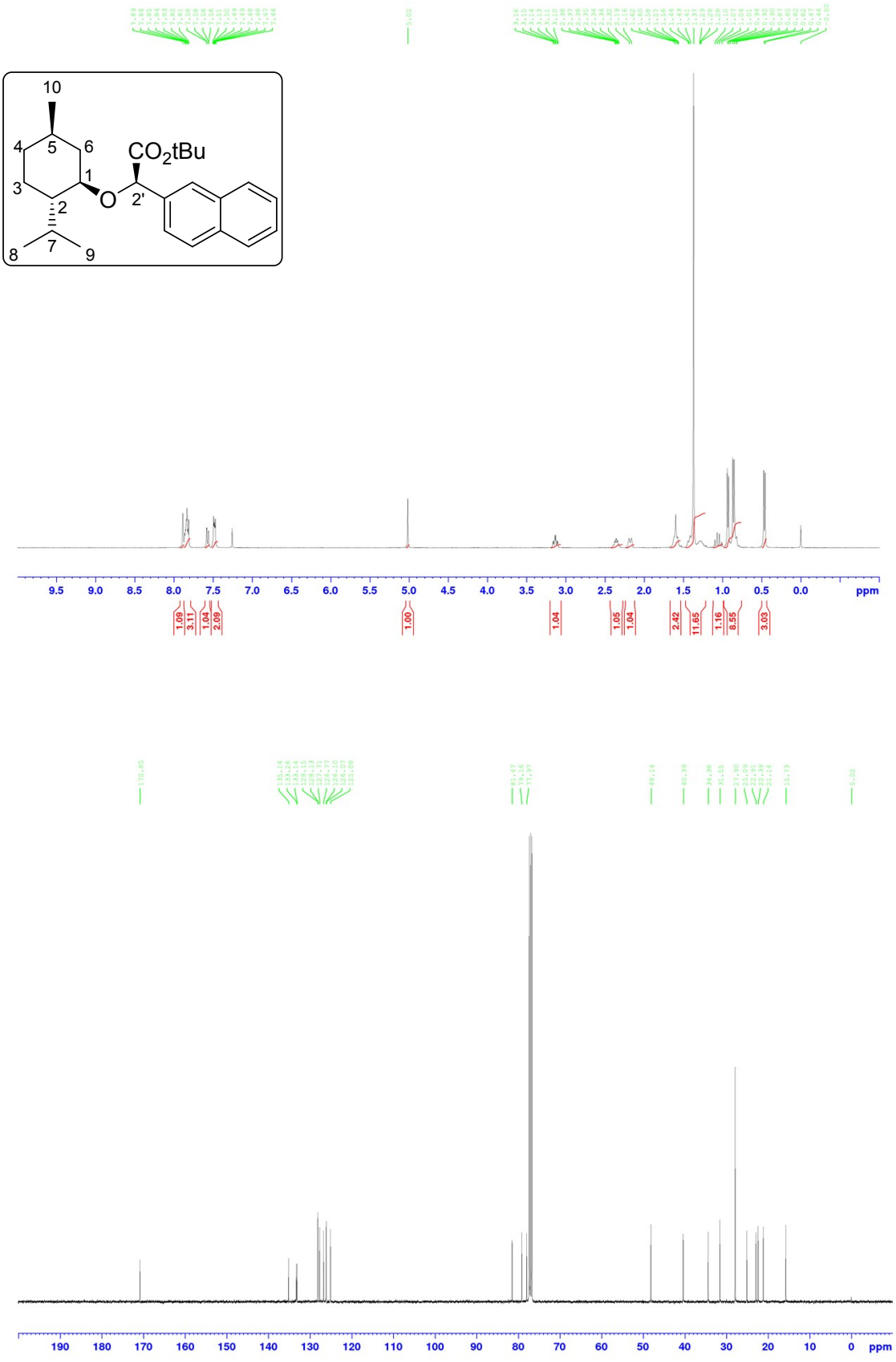

Figure 8. ^{1}H and ^{13}C NMR data for (2′*R*)-^{t}Bu, **4b**

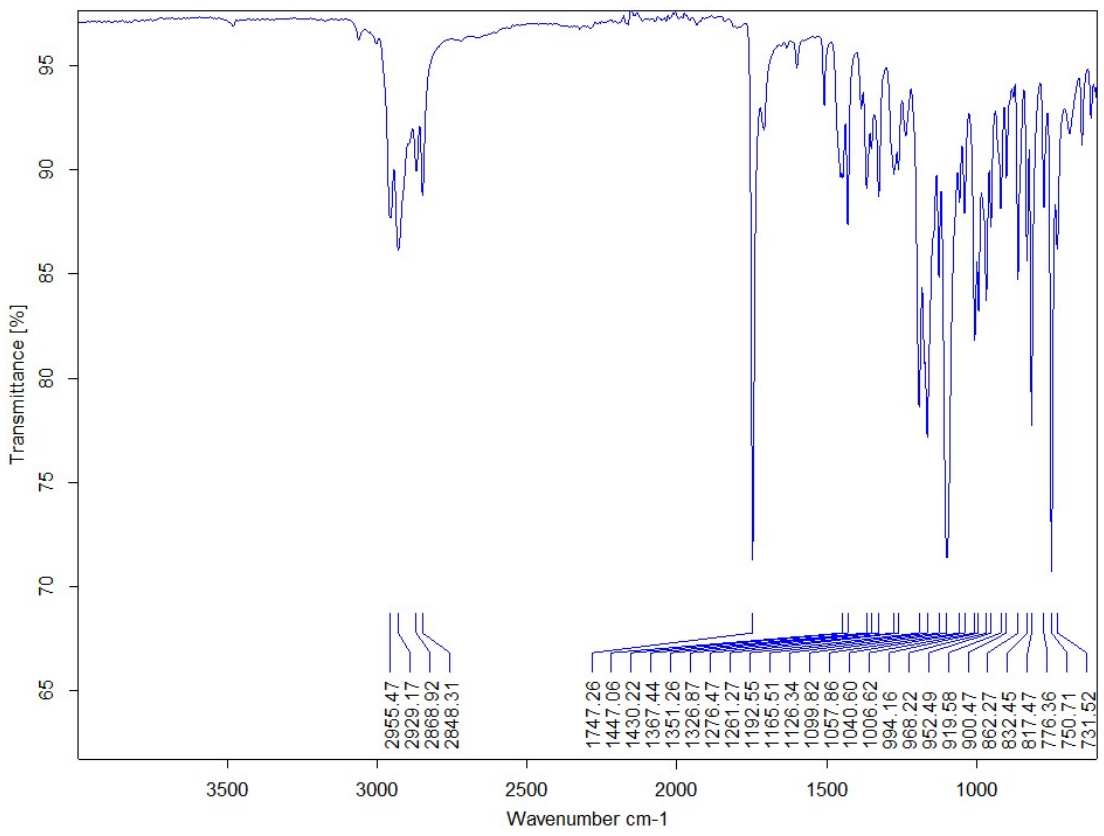

Figure 9. IR data for (2´*S*)-Me **1a**

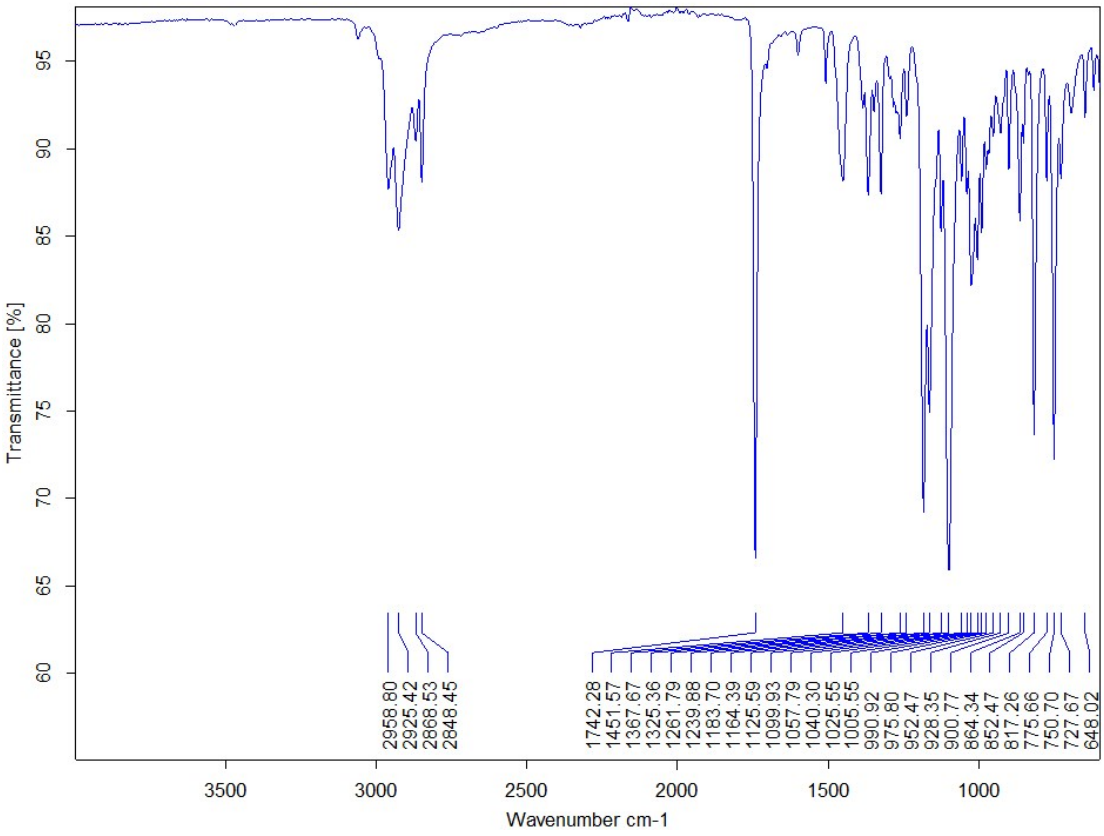

Figure 10. IR data for (2´*S*)-Et **2a**

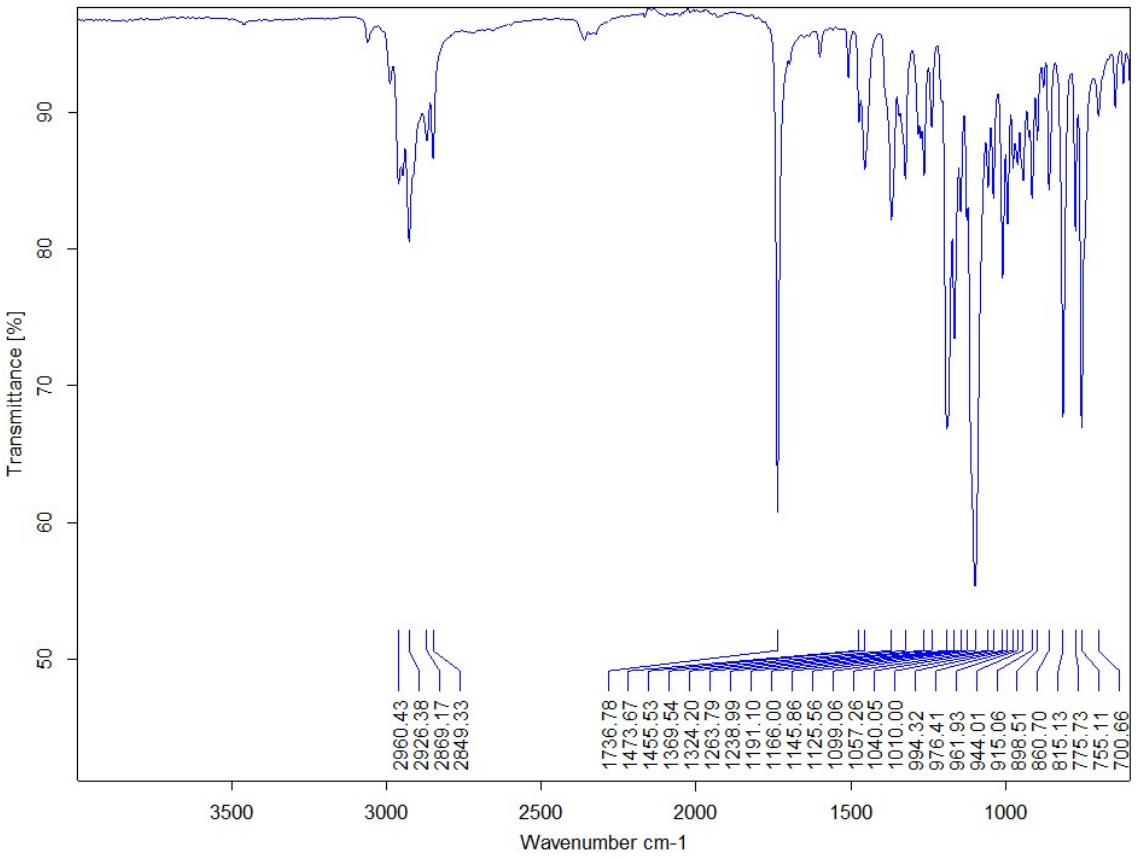

Figure 11. IR data for (2´*S*)-*i*Pr **3a**

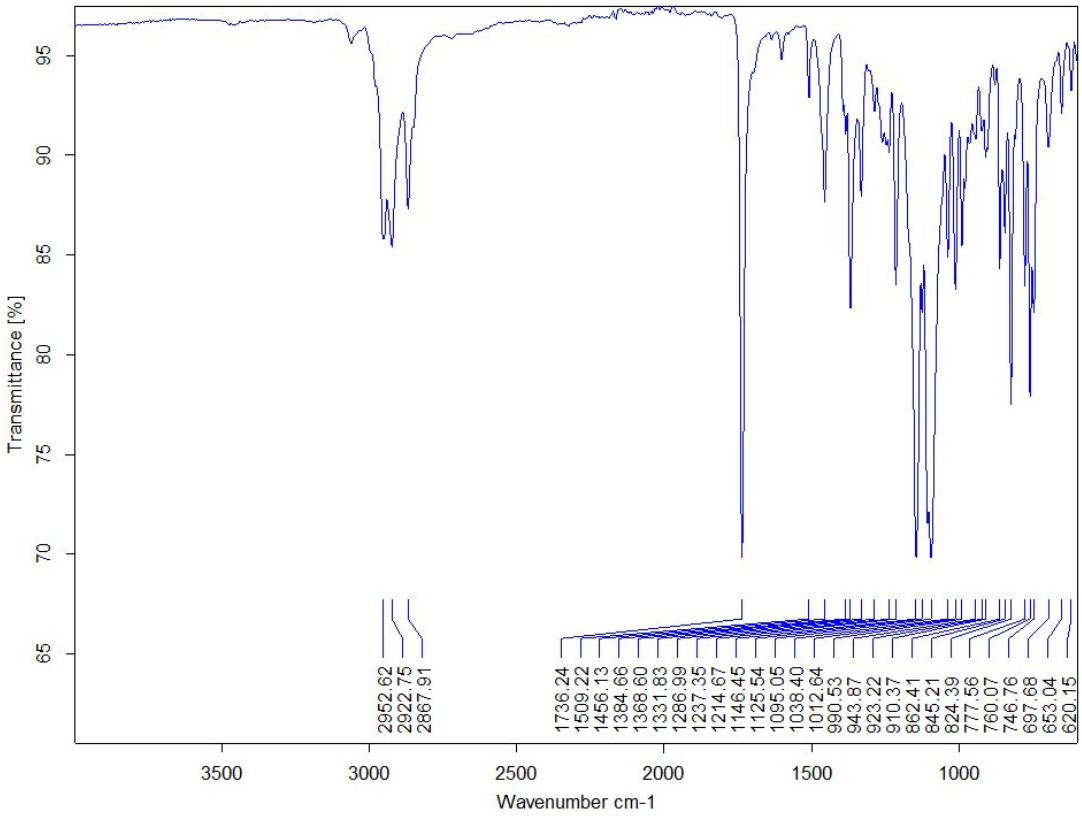

Figure 12. IR data for (2´*S*)-*t*Bu **4a**

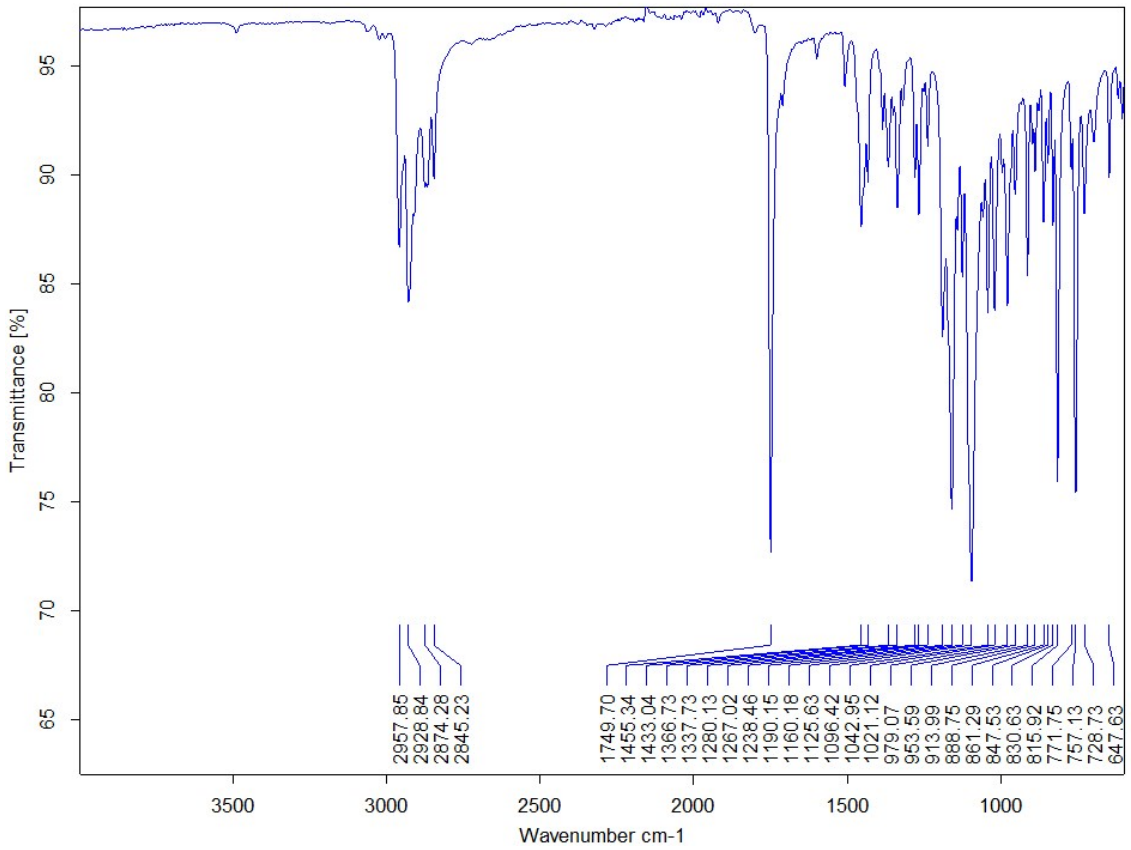

Figure 13. IR data for (2´*R*)-Me **1b**

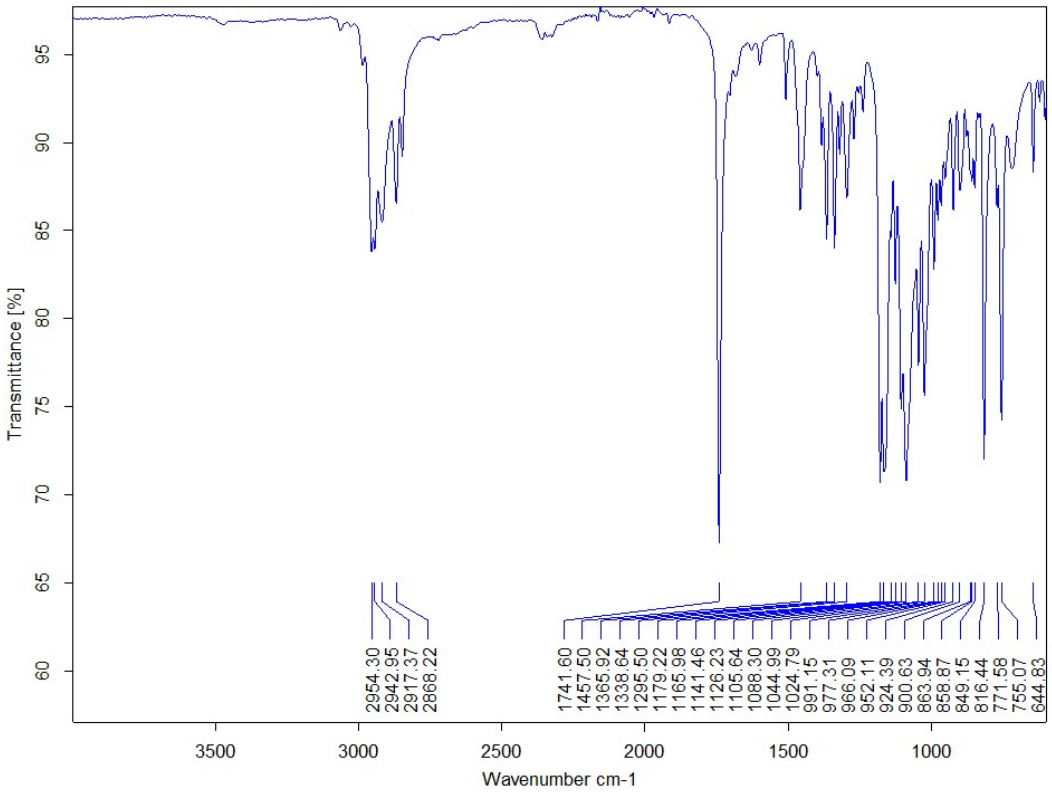

Figure 14. IR data for (2´*R*)-Et **2b**

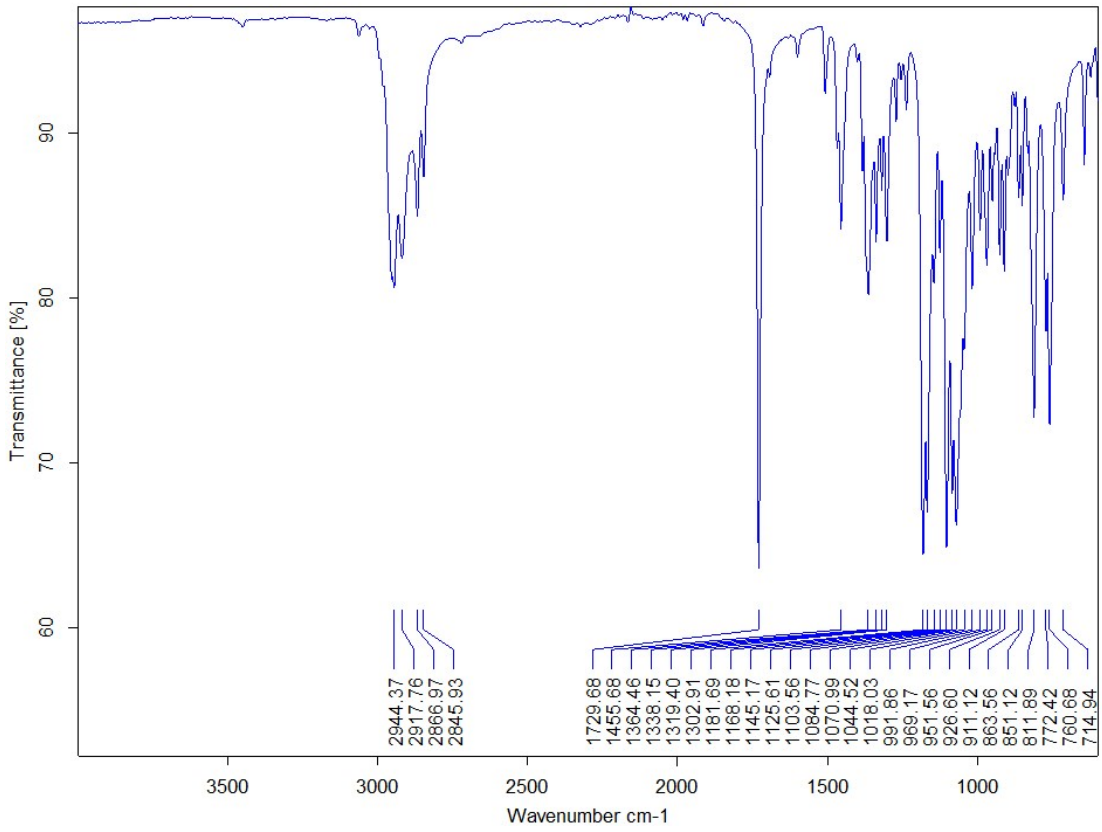

Figure 15. IR data for (2´*R*)-^{i}Pr **3b**

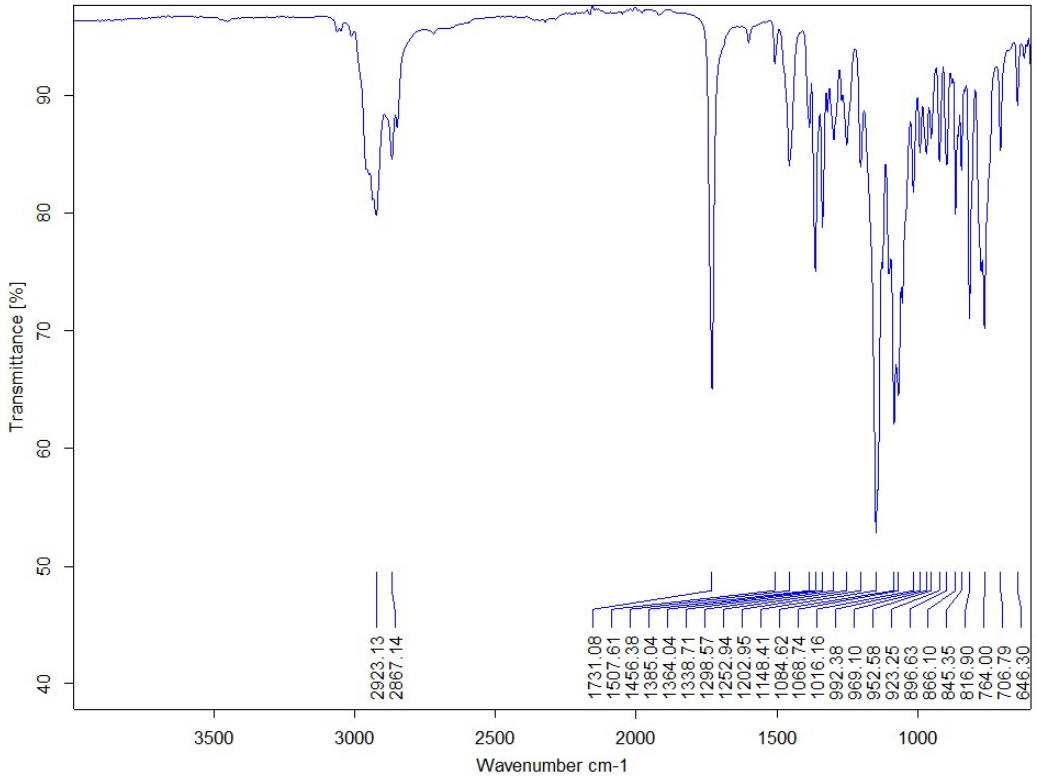

Figure 16. IR data for (2´*R*)-^{t}Bu **4b**

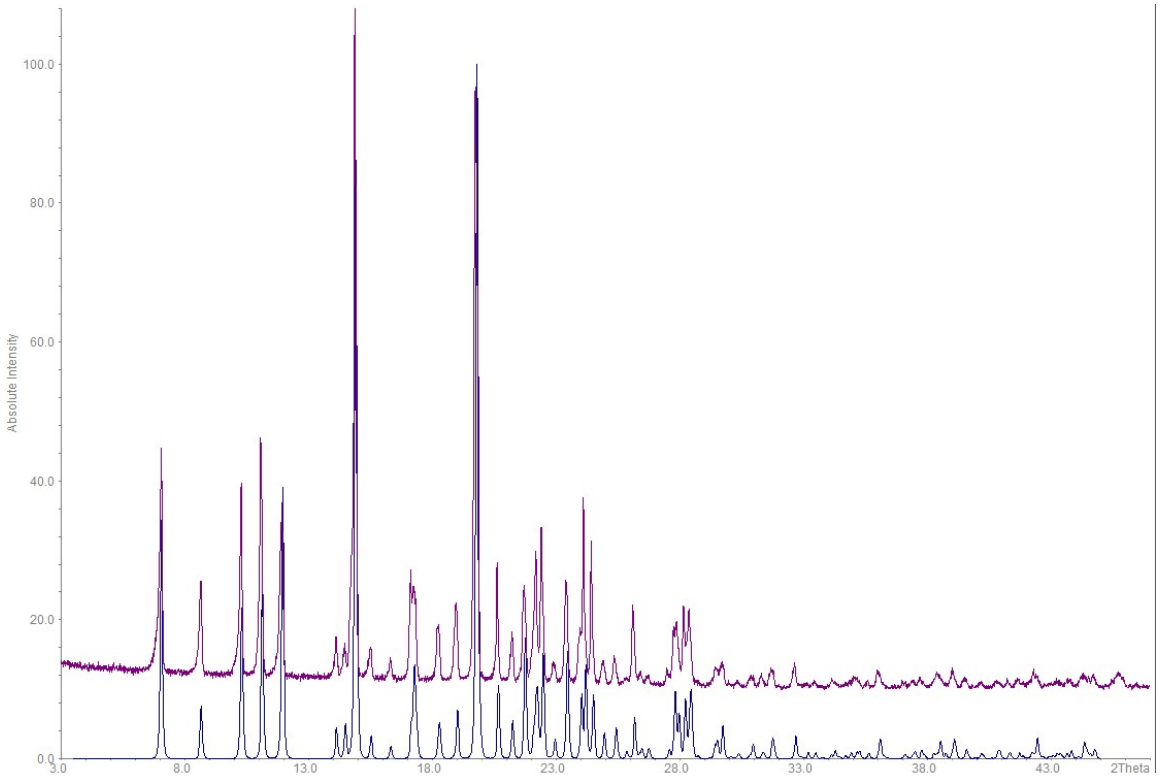

Figure 17. Theoretical (blue) and experimental (magenta) PXRD comparison for (2′*S*)-Me **1a**

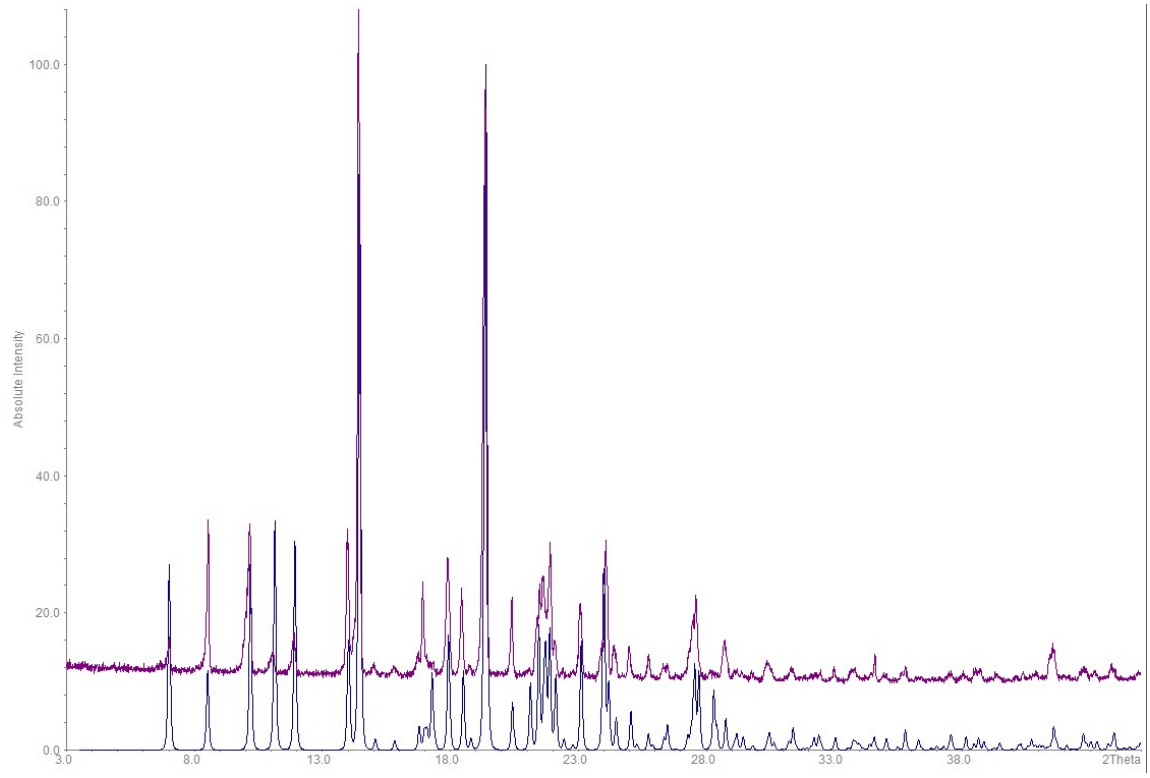

Figure 18. Theoretical (blue) and experimental (magenta) PXRD comparison for (2′*S*)-Et **2a**

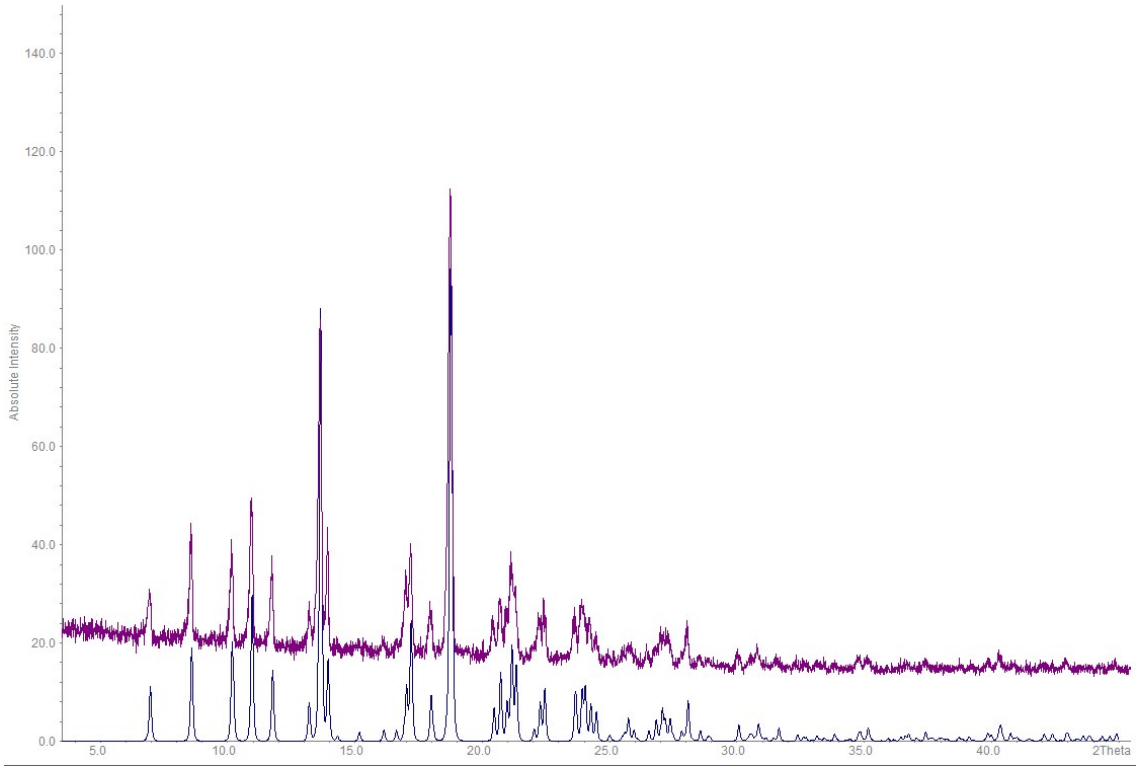

Figure 19. Theoretical (blue) and experimental (magenta) PXRD comparison for (2′*S*)-^{i}Pr **3a**

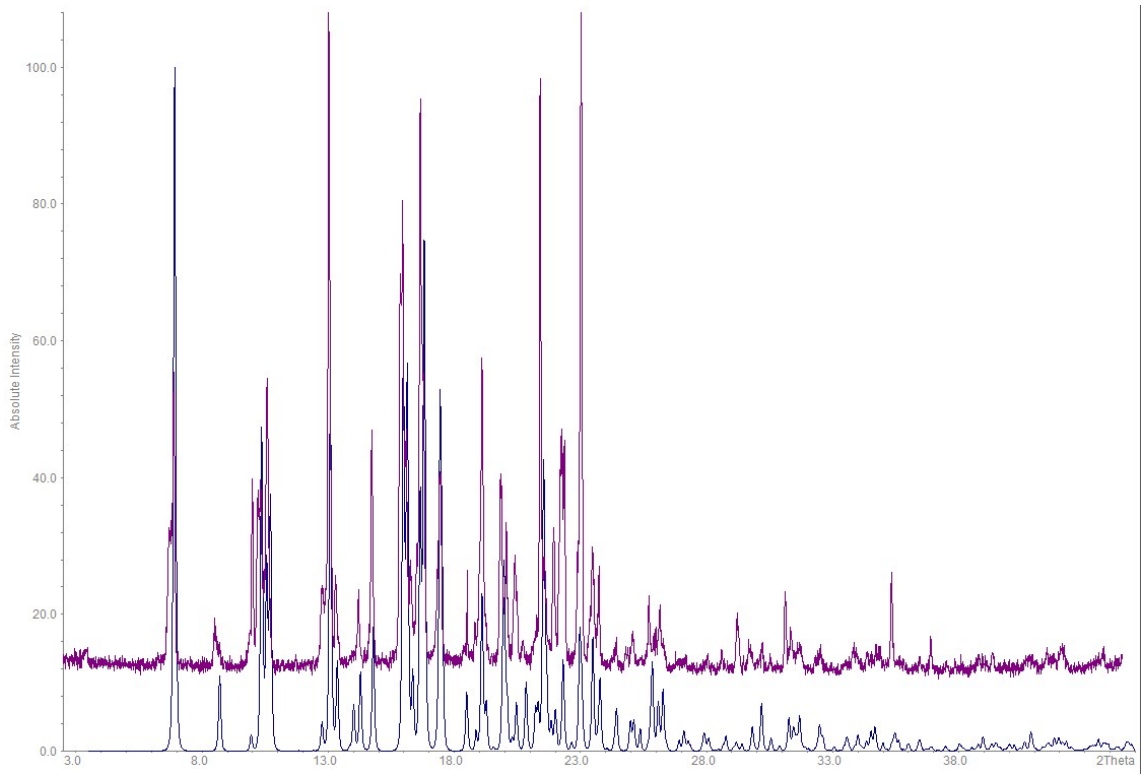

Figure 20. Theoretical (blue) and experimental (magenta) PXRD comparison for (2′*S*)-^{t}Bu **4a**

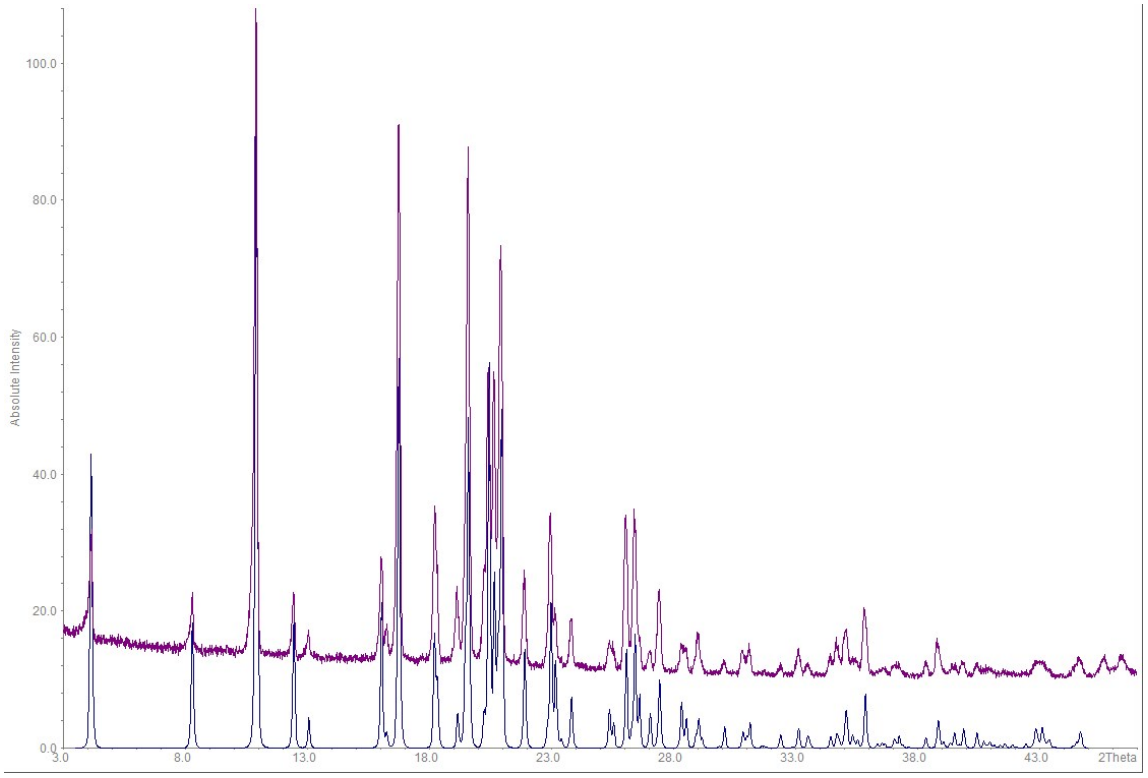

Figure 21. Theoretical (blue) and experimental (magenta) PXRD comparison for (2′*R*)-Me **1b**

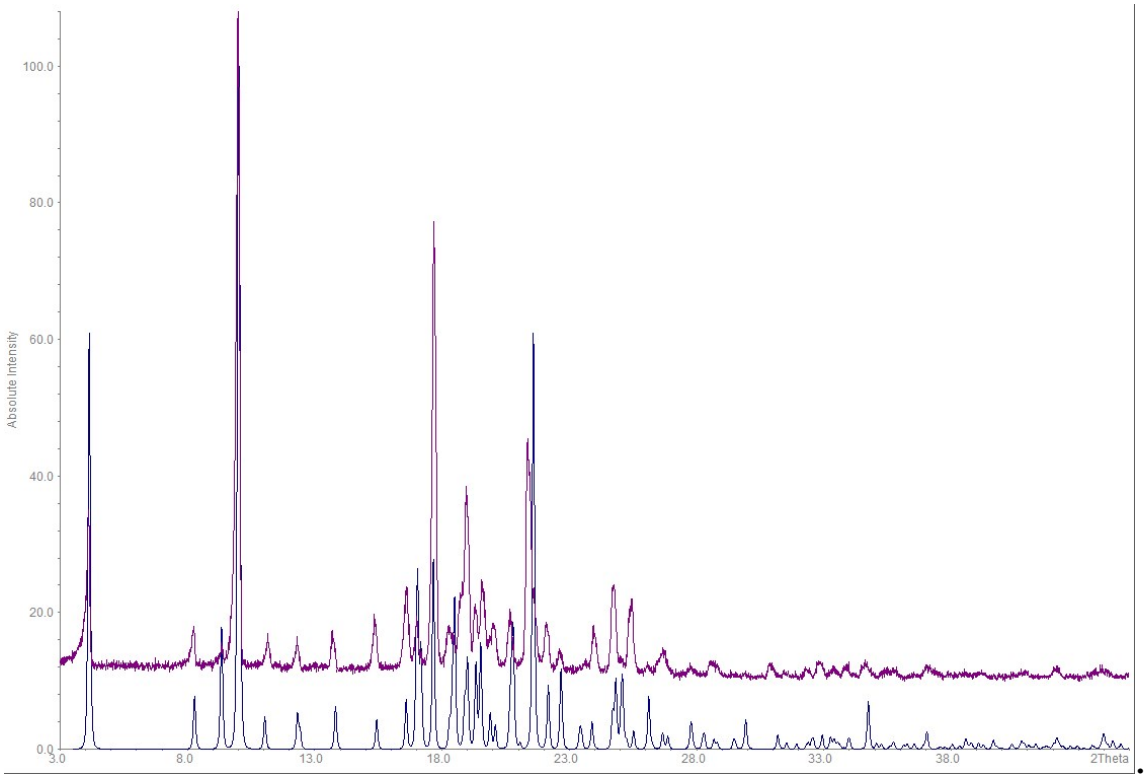

Figure 22. Theoretical (blue) and experimental (magenta) PXRD comparison for (2′*R*)-Et **2b**

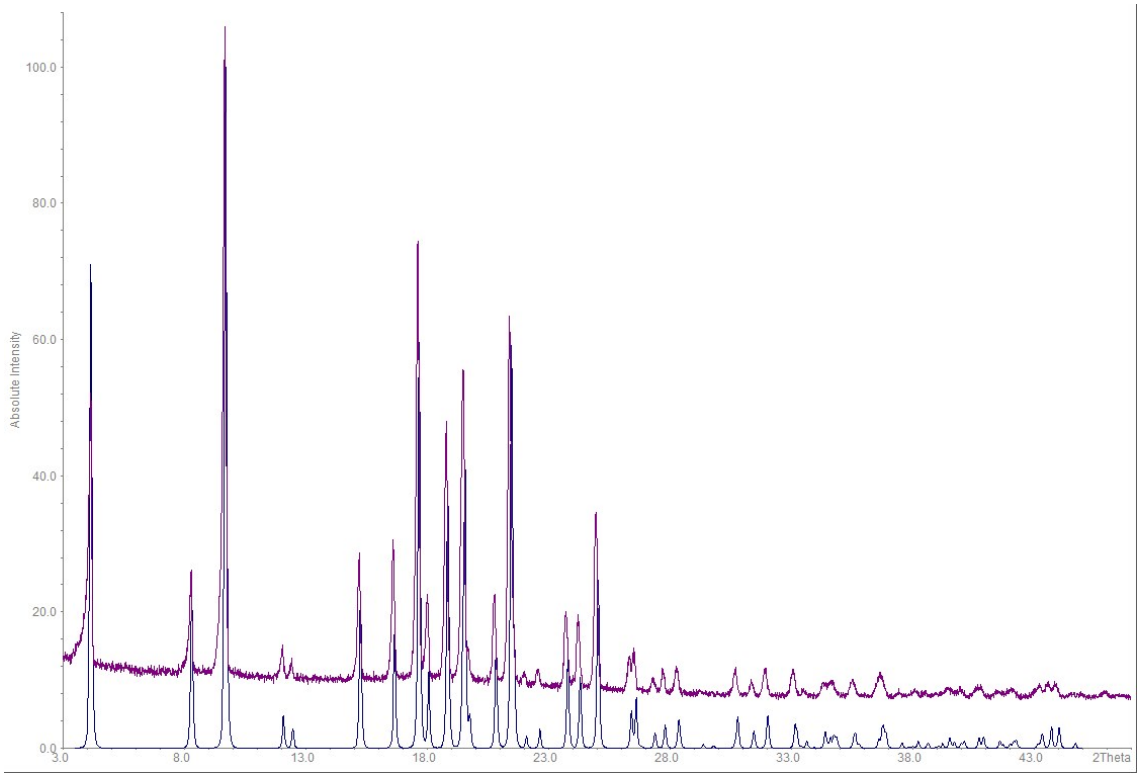

Figure 23. Theoretical (blue) and experimental (magenta) PXRD comparison for (2′*R*)-^{i}Pr **3b**

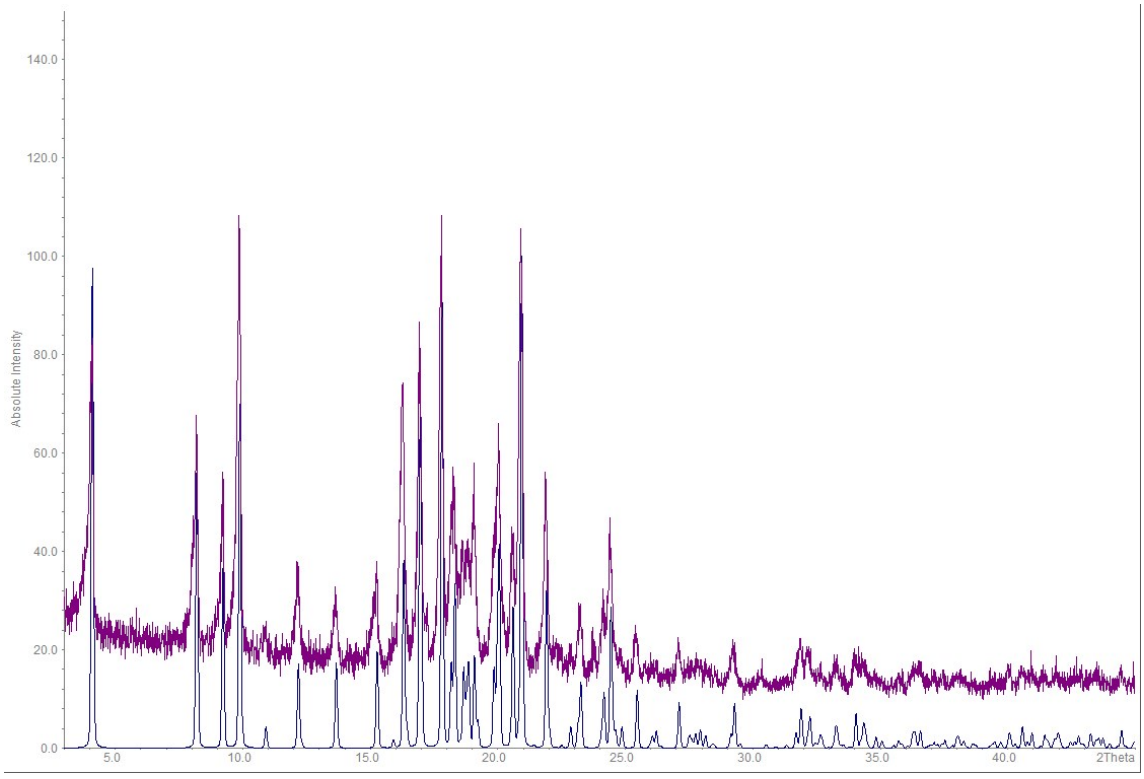

Figure 24. Theoretical (blue) and experimental (magenta) PXRD comparison for (2′*R*)-^{t}Bu **4b**

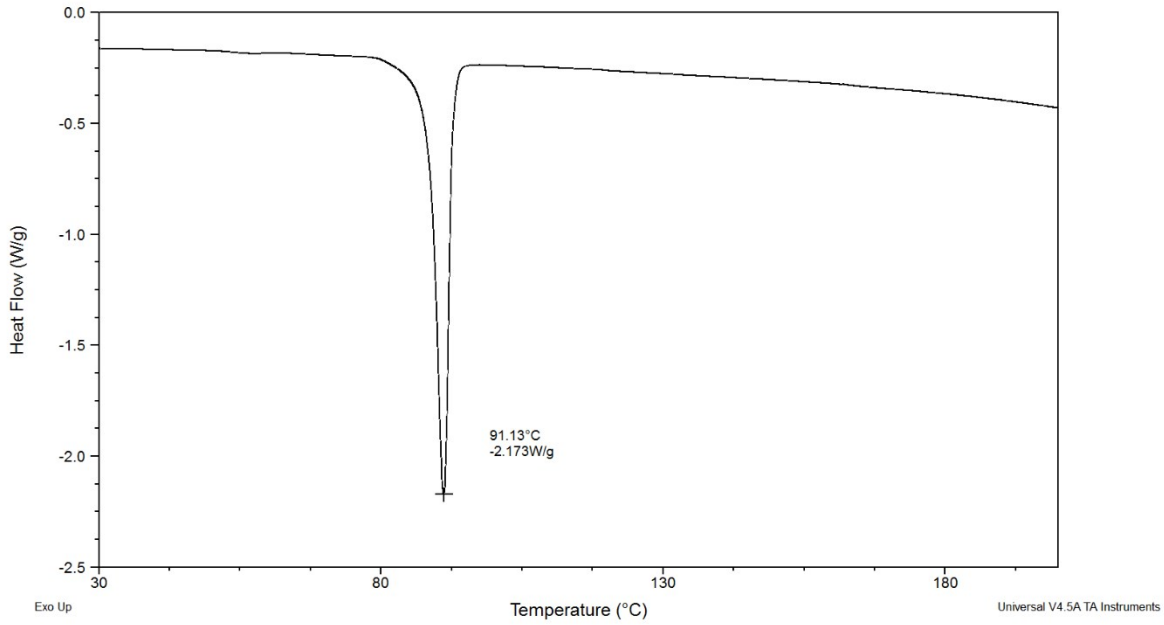

Figure 25. DSC data of (2′*S*)-Me **1a**

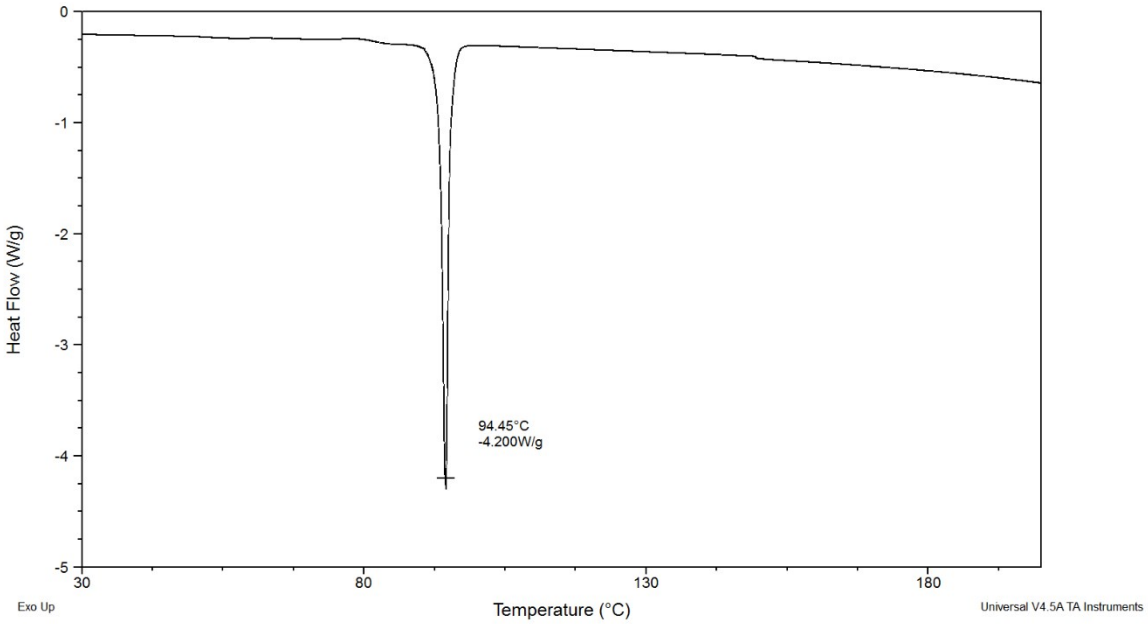

Figure 26. DSC data of (2′*S*)-Et **2a**

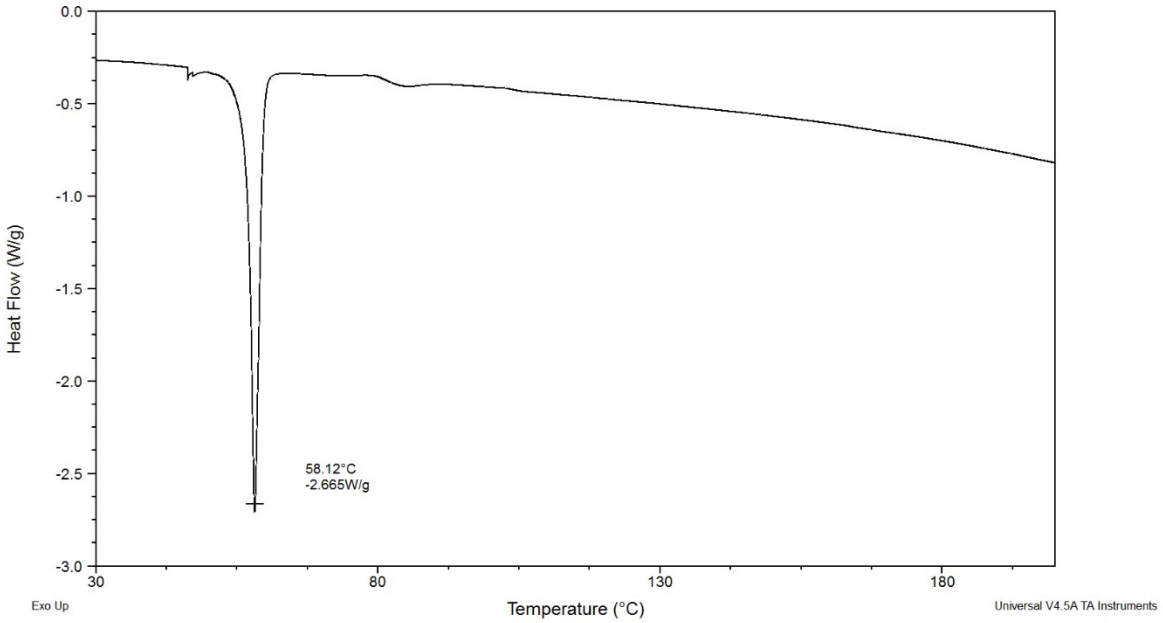

Figure 27. DSC of (2´*S*)-^{i}Pr **3a**

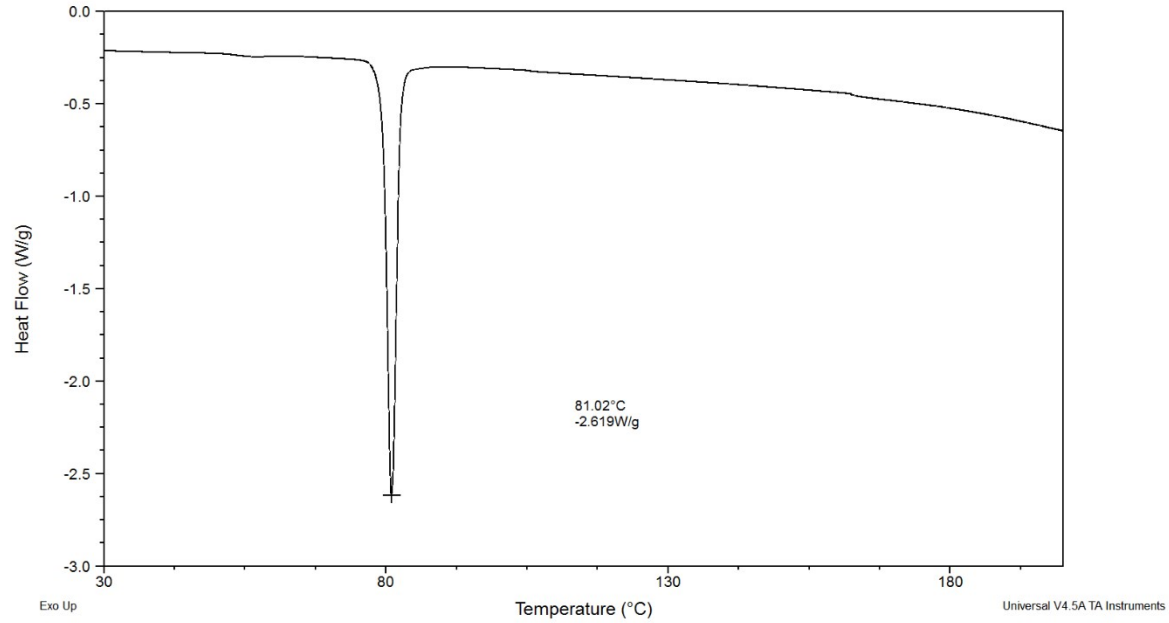

Figure 28. DSC data of (2´*S*)-^{t}Bu **4a**

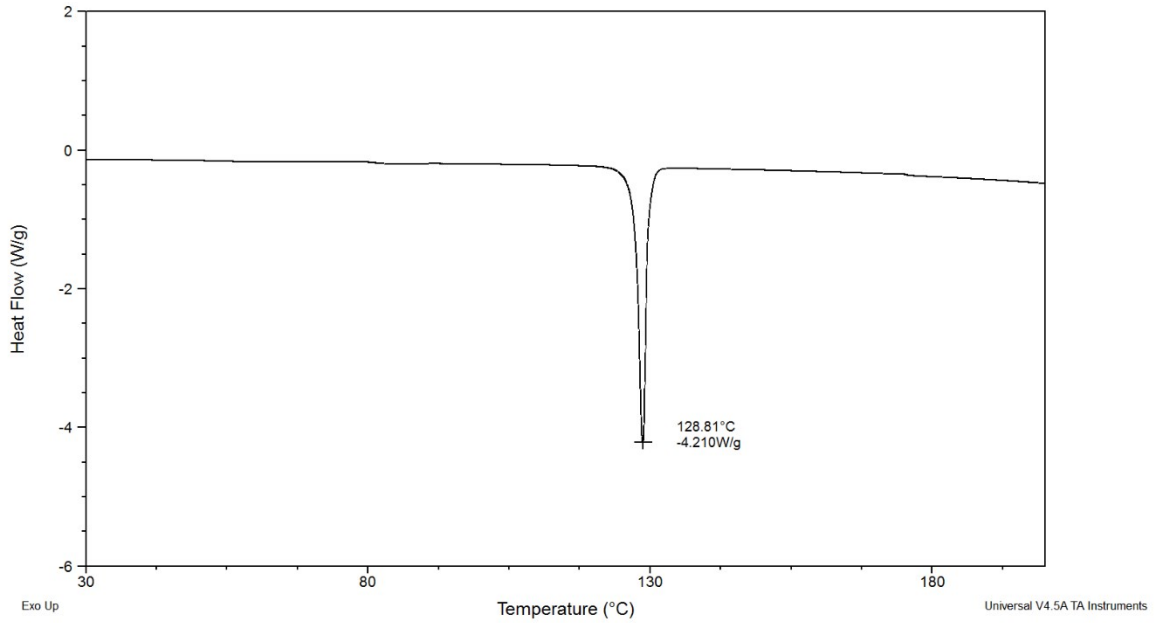

Figure 29. DSC data of (2′*R*)-Me **1b**

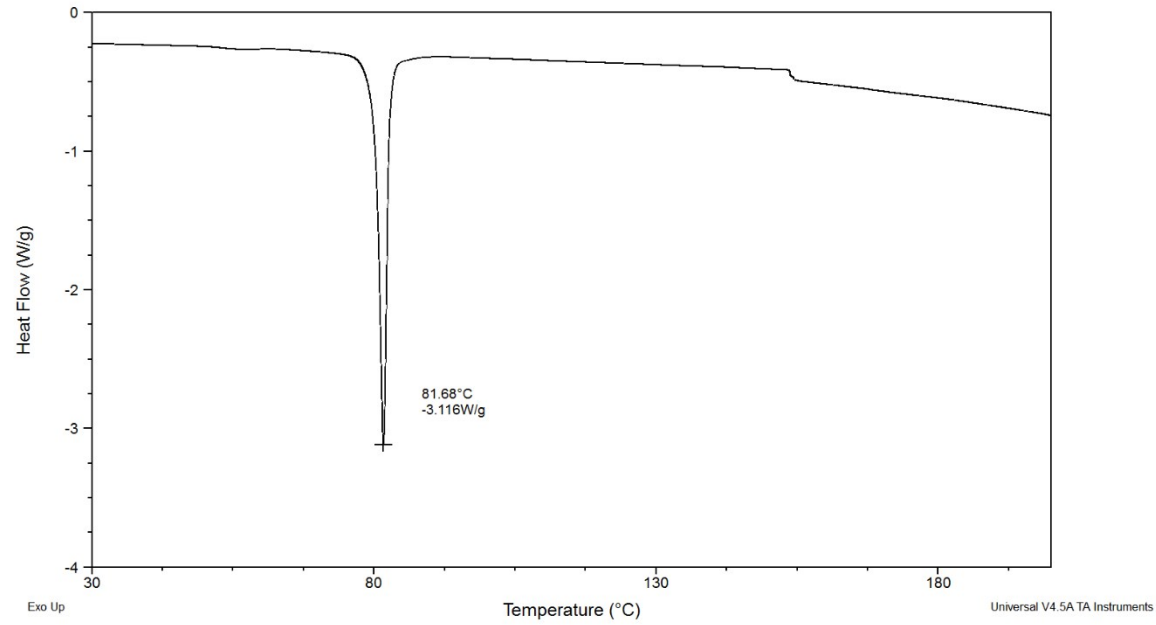

Figure 30. DSC data of (2′*R*)-Et **2b**

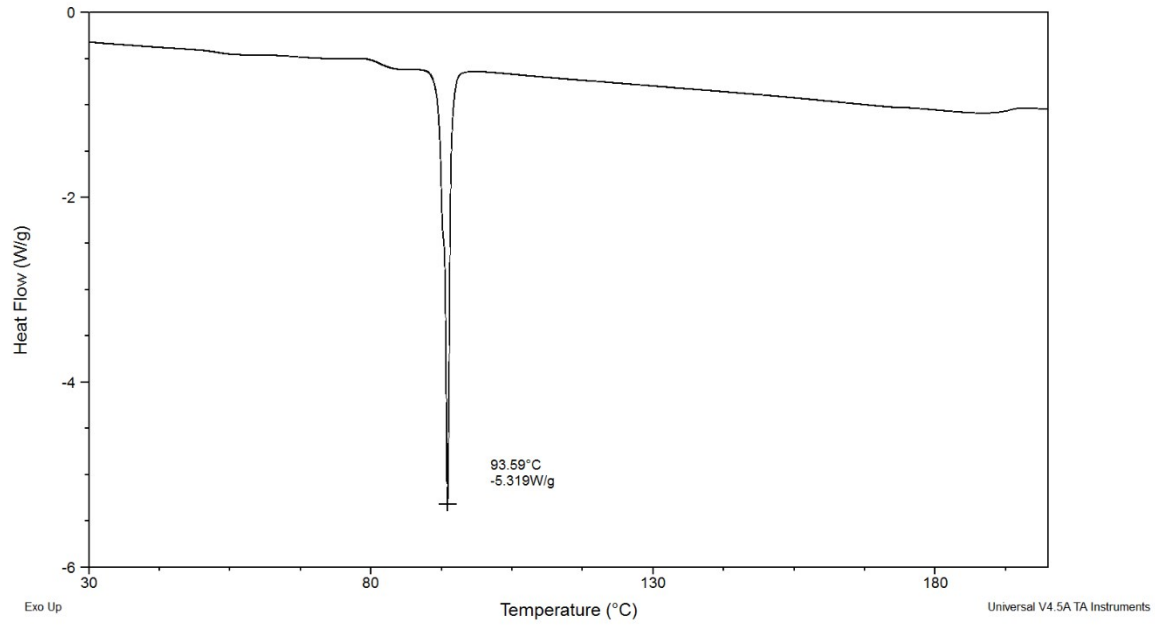

Figure 31. DSC data of (2′*R*)-^{i}Pr **3b**

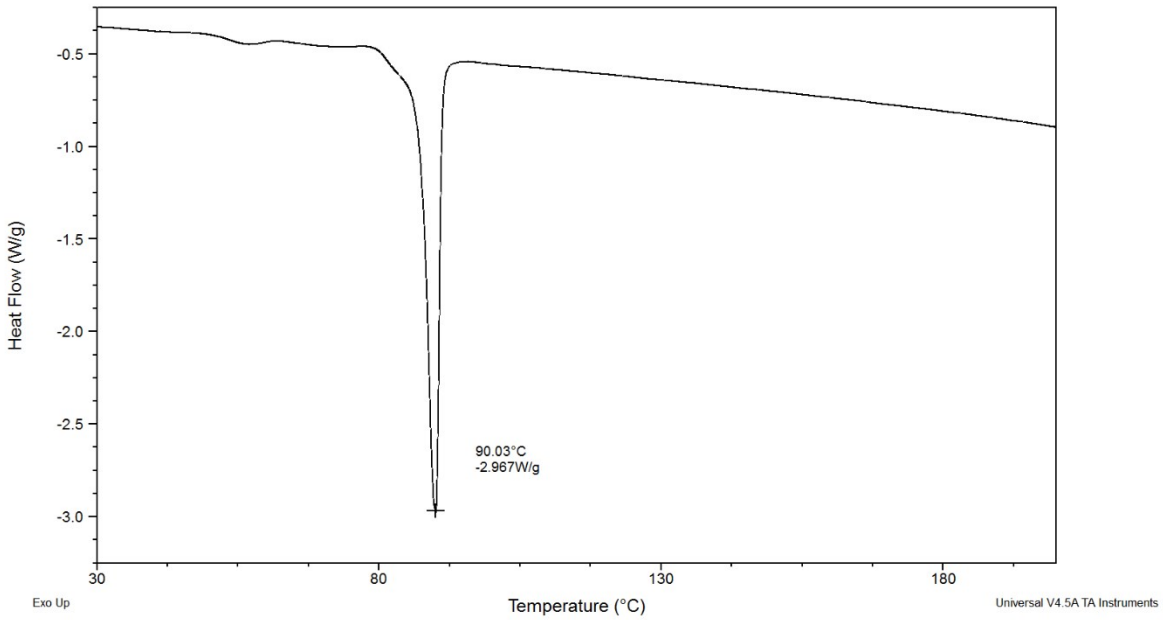

Figure 32. DSC data of of (2′*R*)-^{t}Bu **4b**

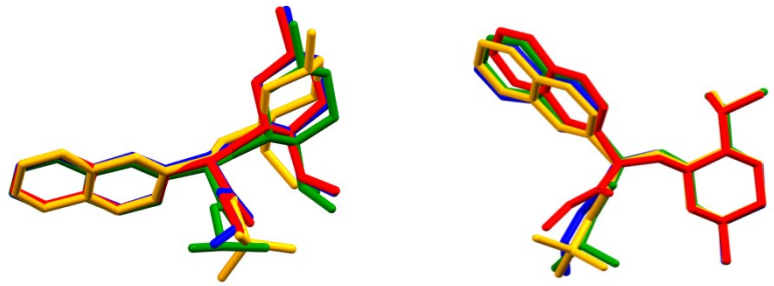

Figure 33. Superimposition of a molecule from each compound in the series of the brittle **1a-4a** (left) and ductile **1b-4b** (right) compounds, showing the relative orientation of the menthyl and ester groups. [Red: R = Me, Blue: R = Et, Green: R = ^{i}Pr, Orange: R = ^{t}Bu.]

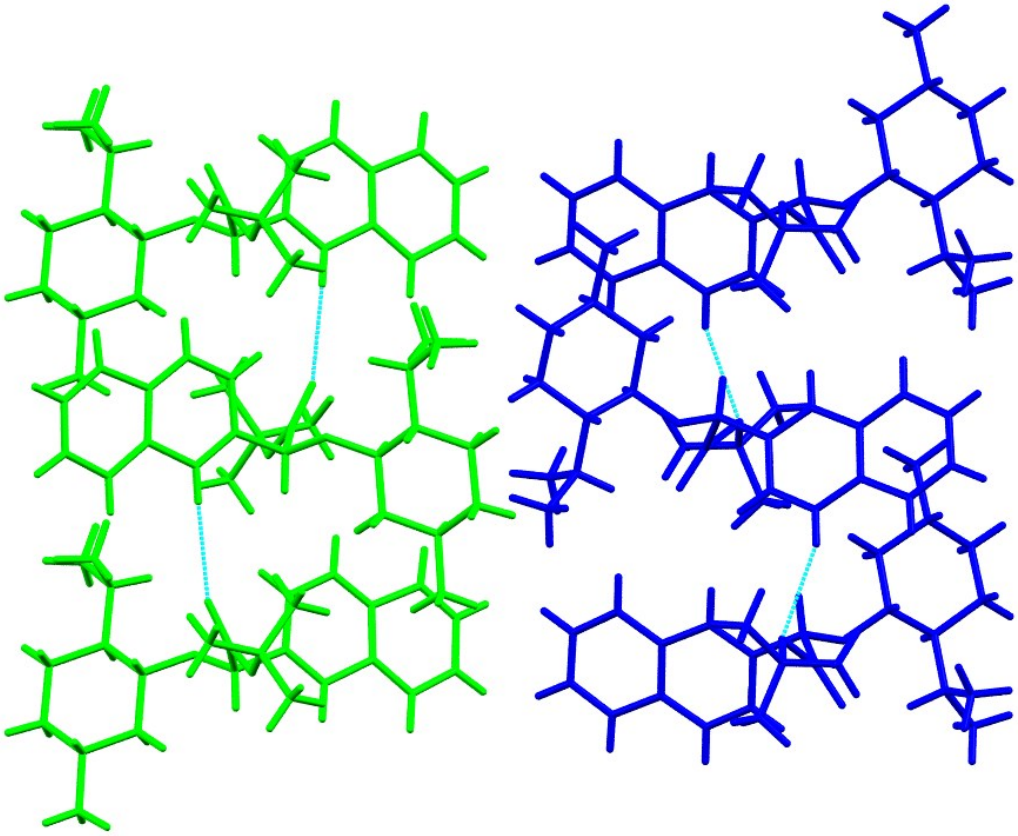

Figure 34. The H…H close contacts in (2′*S*)-^{t}Bu (**4a**) viewed down the *a* axis, right. Colours blue and green indicate the symmetry equivalent molecules.

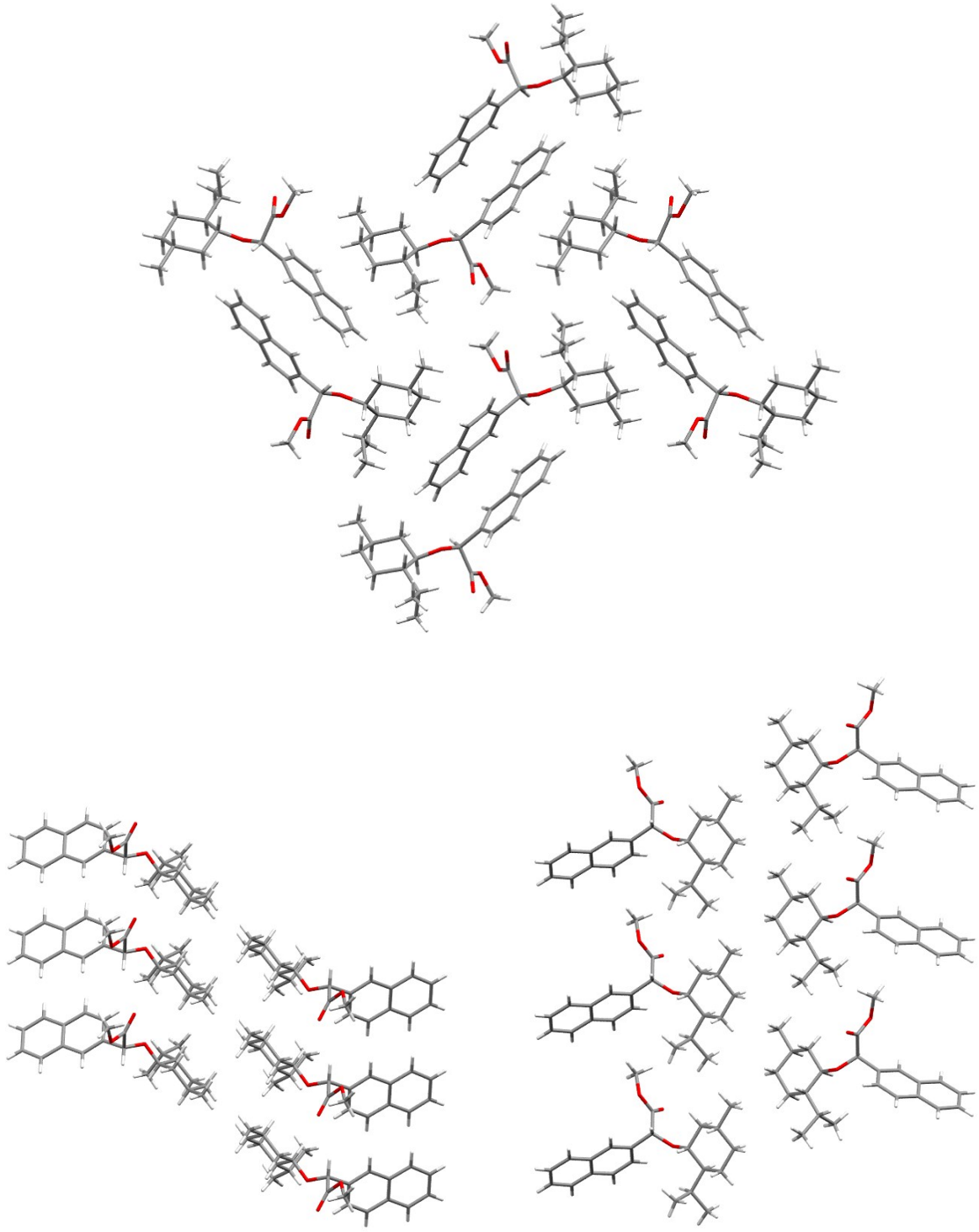

Figure 35. View down the *a*-axis showing the interdigitation of molecules in (2′*S*)-Me (**1a**), top. View down the *b*-axis, bottom left, and down the *a*-axis, bottom right, showing likely slip plane in (2′*R*)-Me (**1b**). Nanoindentation studies were not possible on crystals of **1b**, so slip planes not experimentally confirmed.

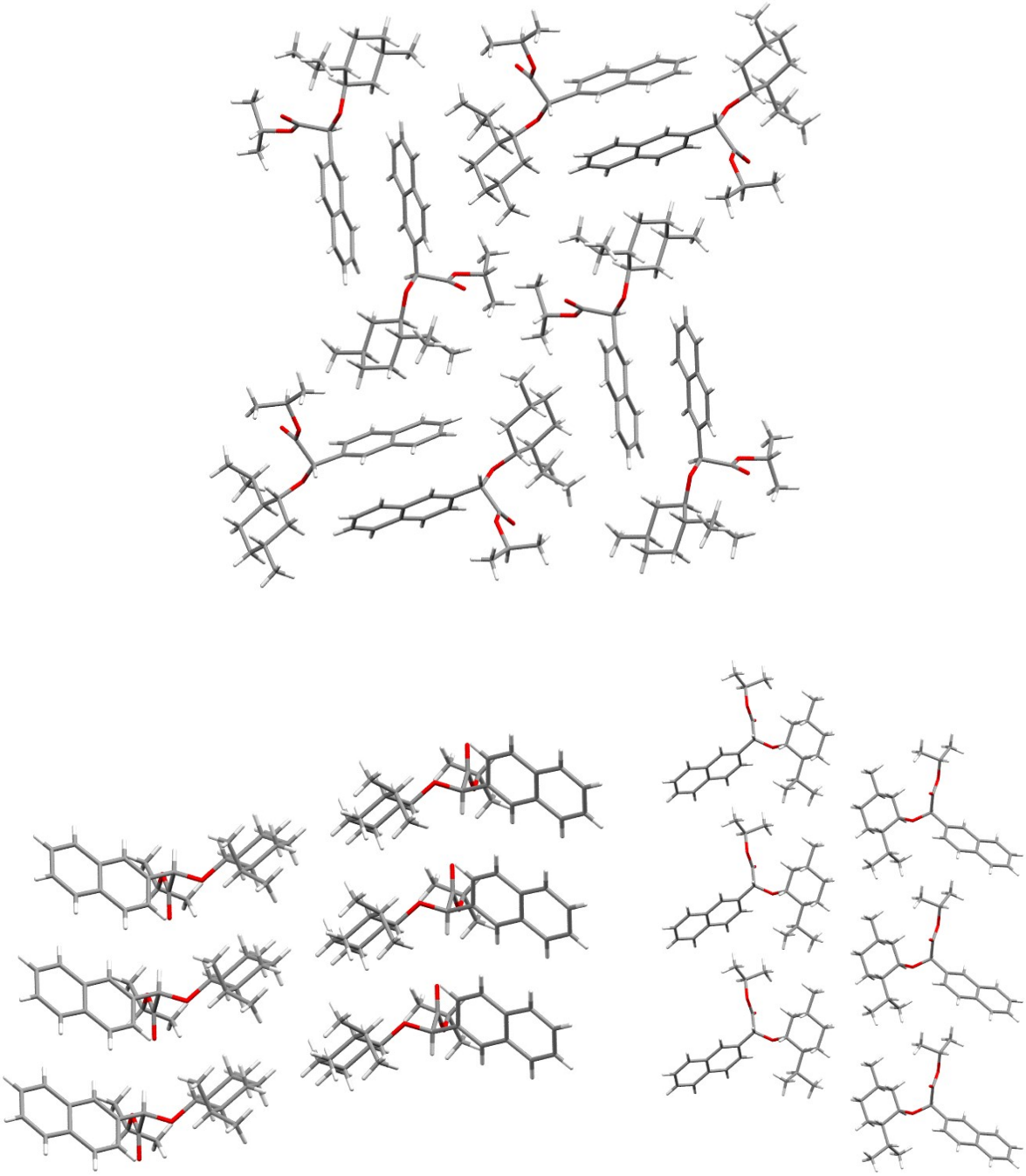

Figure 36. View down the *a*-axis showing the interdigitation of molecules in (2′*S*)-^{i}Pr (**3a**), top. View down the *b*-axis, bottom left, and down the *a*-axis, bottom right, showing the slip plane in (2′*R*)-^{i}Pr (**3b**).

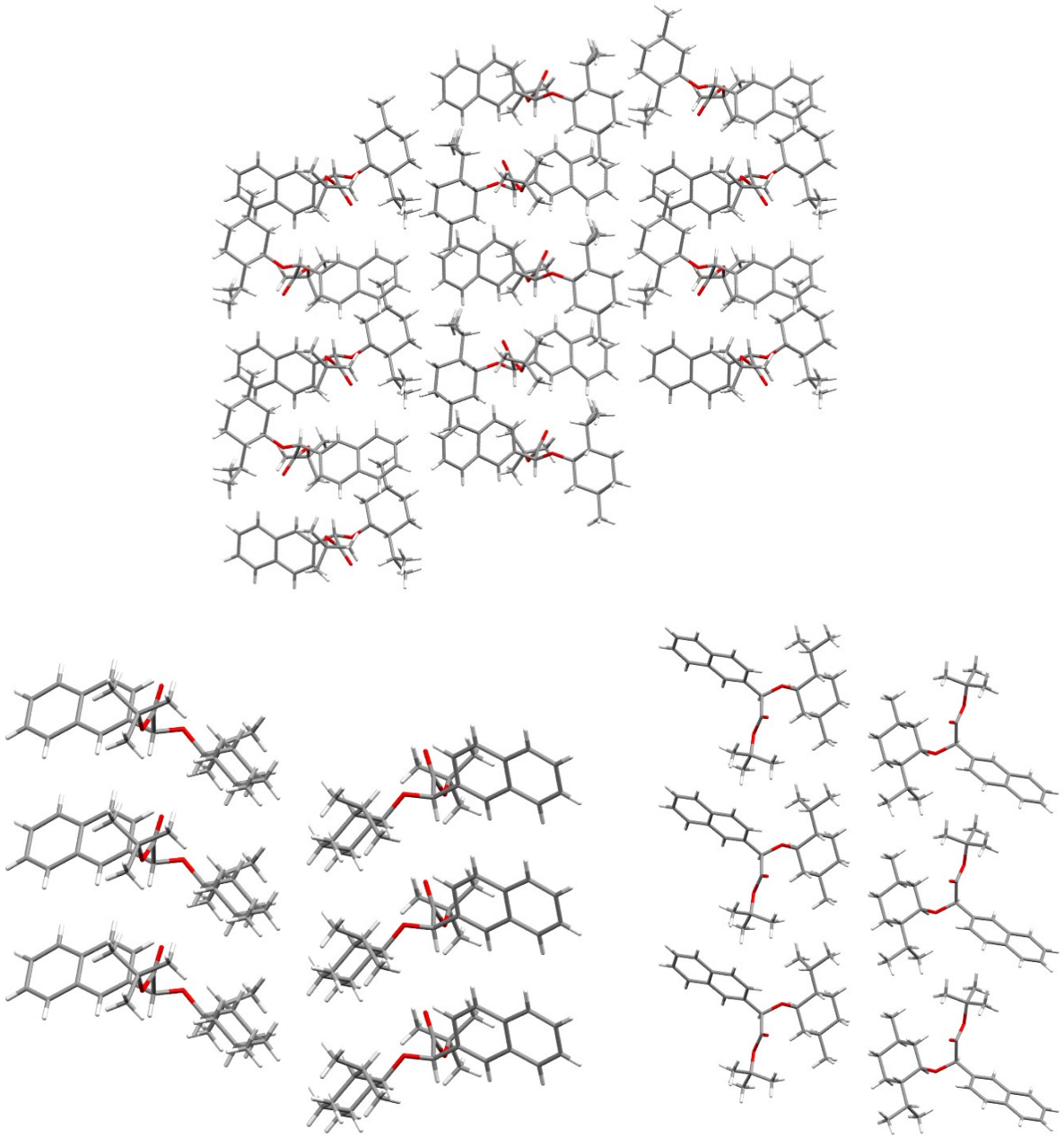

Figure 37. View down the *a*-axis showing the interdigitation of molecules in (2′*S*)-^{t}Bu (**4a**), top. View down the *b*-axis, bottom left, and down the *a*-axis, bottom right, showing the slip plane in (2′*R*)-^{t}Bu (**4b**).

(2′*S*)-Me **1a**

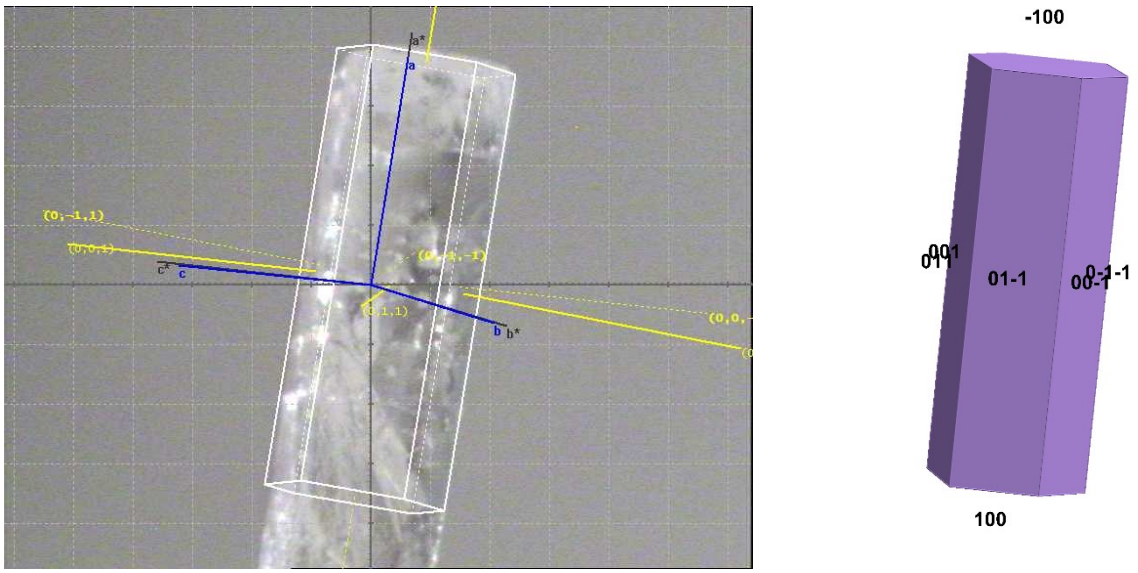

Figure 38. Crystal on the diffractometer and crystal shape drawn using the exported P4P file

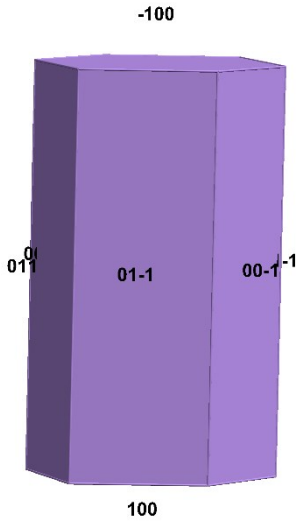

Figure 39. Crystal shape calculated using the Eatt values.

FACE	Slice Att.Energy
1 0 0	-22.34
0 1 -1	-12.53
0 1 1	-12.53
0 0 1	-11.81

There is reasonable agreement here between Eatt Xtal and observed Xtal.

(2′*R*)-Me **1b**

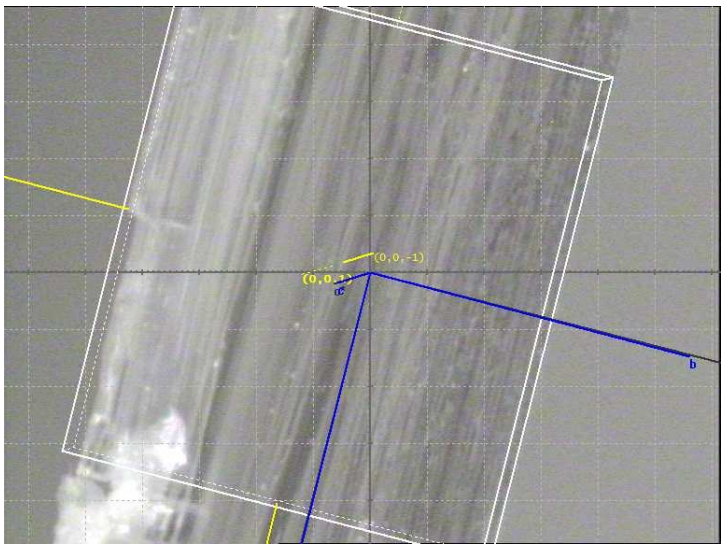

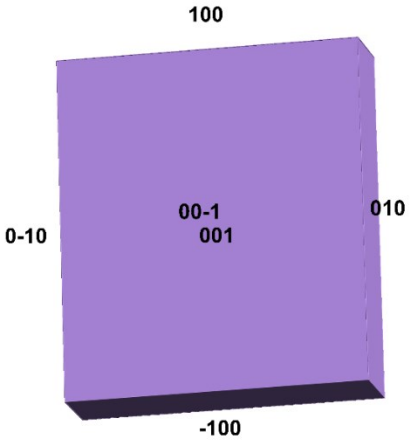

Figure 40. Crystal on the diffractometer and crystal drawn using the exported P4P file

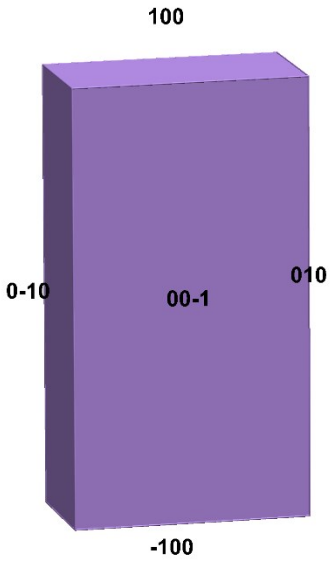

Figure 41. Crystal shape calculated using the Eatt values

FACE	Slice Att.Energy
0 0 1	-8.57
1 0 0	-29.73
0 1 0	-15.95

There is reasonable agreement here between Eatt Xtal and observed Xtal.

(2′*S*)-Et **2a**

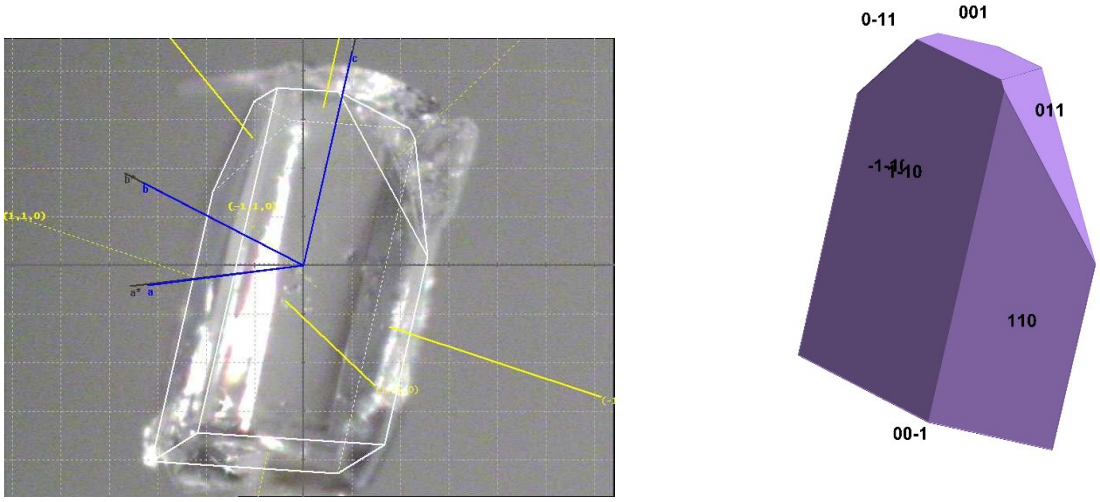

Figure 42. Crystal on the diffractometer and crystal drawn using the exported P4P file

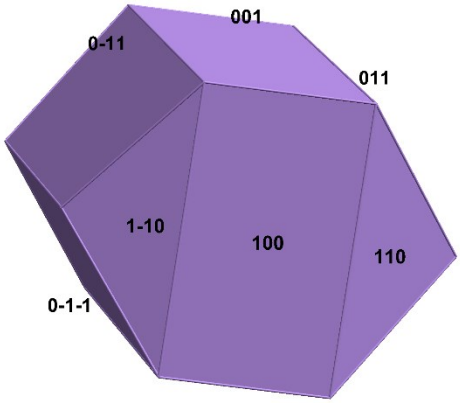

Figure 43. Crystal shape calculated using the Eatt values

FACE	Slice Att.Energy
1 1 0	-24.13
1 -1 0	-24.12
0 1 1	-15.03
1 0 0	-22.72
0 0 1	-14.05

This crystal was difficult to index. Note that the calculation assumes that a parallelepiped will be adopted. Whilst is not a parallelpipied, the calculated attachment energies are included for consistency.

(2′*R*)-Et **2b**

It was not possible to face index these crystals.

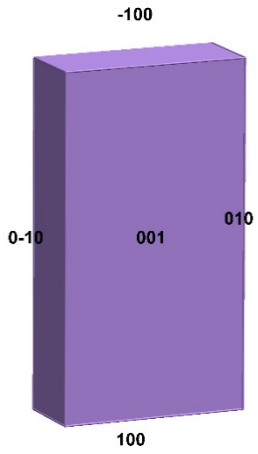

Figure 44. Crystal shape calculated using the Eatt values

FACE	Slice Att.Energy
1 0 0	-20.01
0 1 0	-10.78
0 0 1	-4.45

(2′*S*)-*i*Pr **3a**

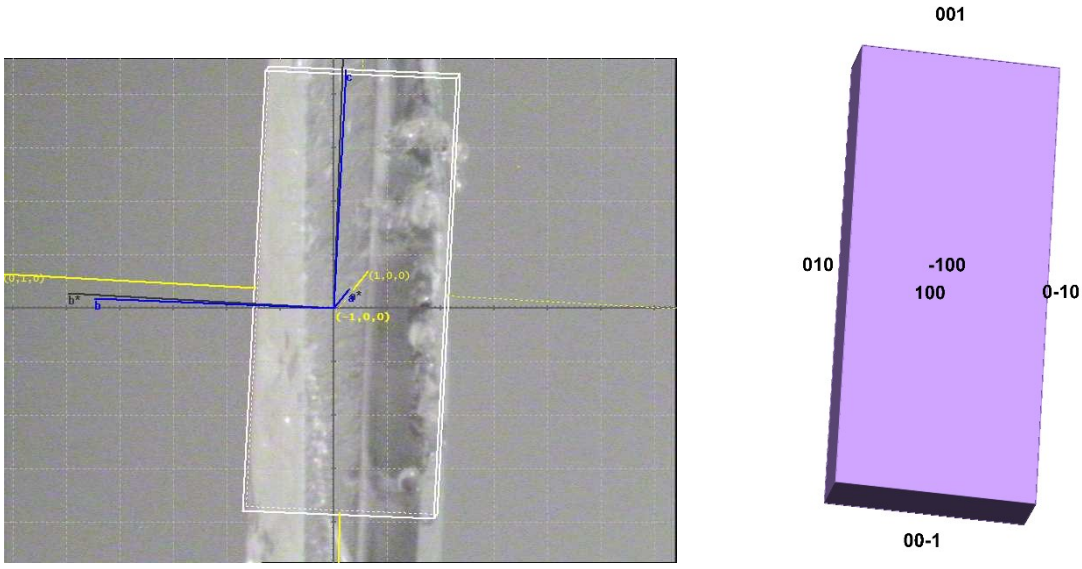

Figure 45. Crystal on the diffractometer and crystal drawn using the exported P4P file

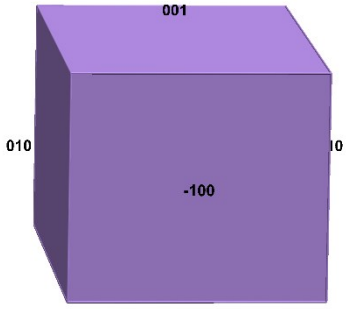

Figure 46. Crystal shape calculated using the Eatt values

FACE	Slice Att.Energy
1 0 0	-22.55
0 1 0	-13.92
0 0 1	-12.41

CELL 7.0826 16.1438 20.5765 90. 90. 90.
b and *c* and their Eatt are similar and more rapid growth in the *a* direction would be expected on the basis of Eatt. Observed growth in the *a* direction is slow and this must be due to kinetic factors.

(2′*R*)-^{i}Pr **3b**

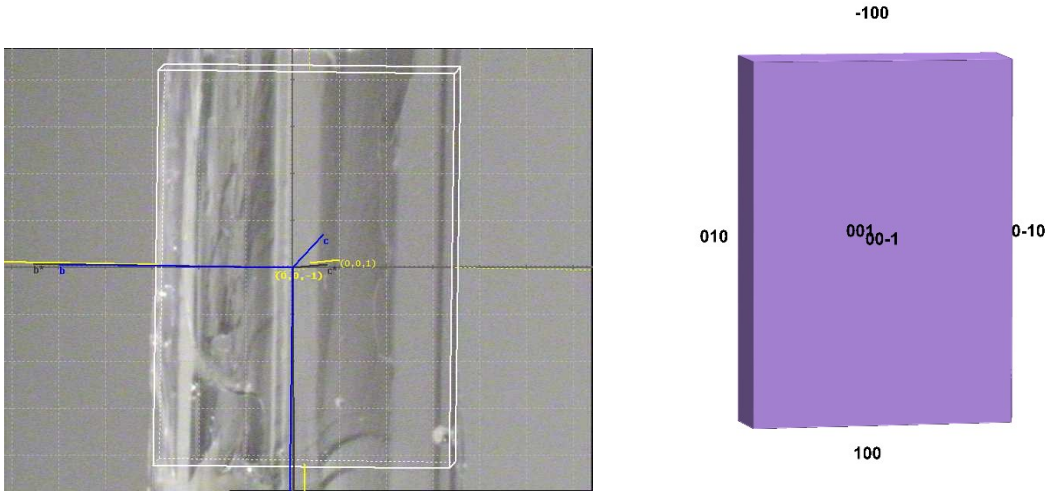

Figure 47. Crystal on the diffractometer and crystal drawn using the exported P4P file

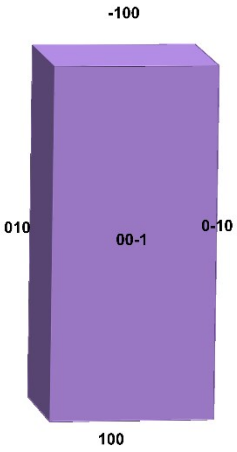

Figure 48. Crystal shape calculated using the Eatt values

FACE	Slice Att.Energy
1 0 0	-31.52
0 1 0	-14.99
0 0 1	-9.10

There is OK agreement here between Eatt Xtal and observed Xtal.

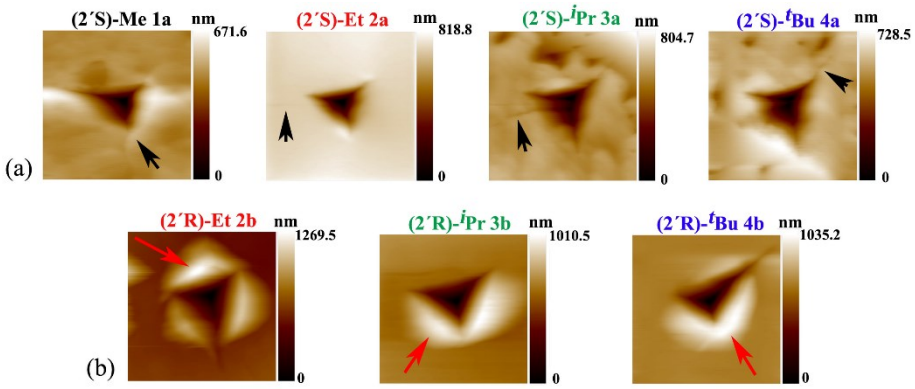

Figure 49. Post-indent AFM scans, 20 µm x 20 µm, of the residual indents of the crystals of (a) **1a**-**4a**, and (b) **2b**-**4b**. Black arrows in (a) show cracks, and red arrows in (b) show pile-up of the material.

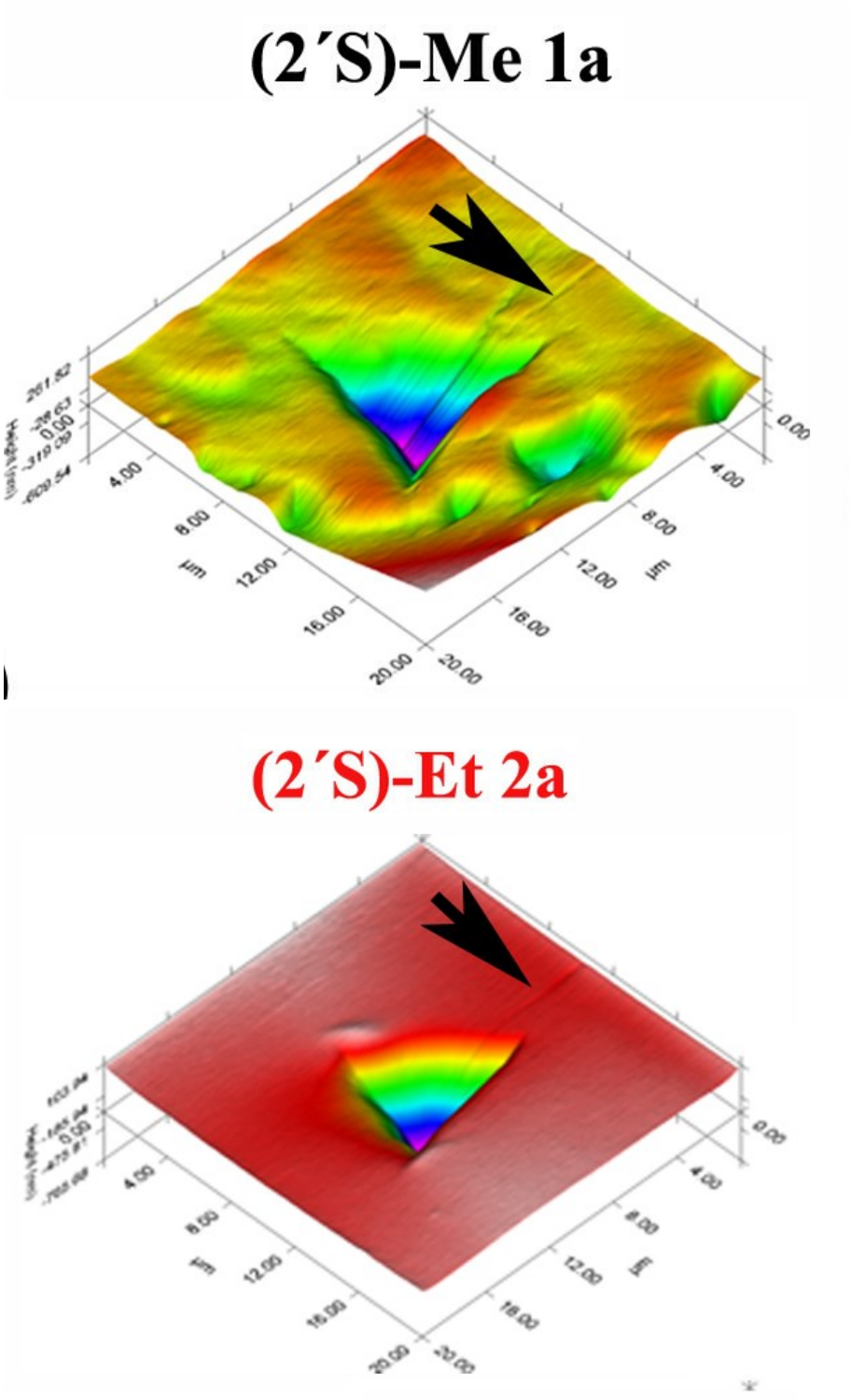

Figure 50. The post-indent AFM scans (3D) of the residual indents of crystals for the (2´*S*)-Me **1a** and (2´*S*)-Et **2a** crystals. The black arrows show cracks. The scan size of all the AFM images is 20 µm x 20 µm.

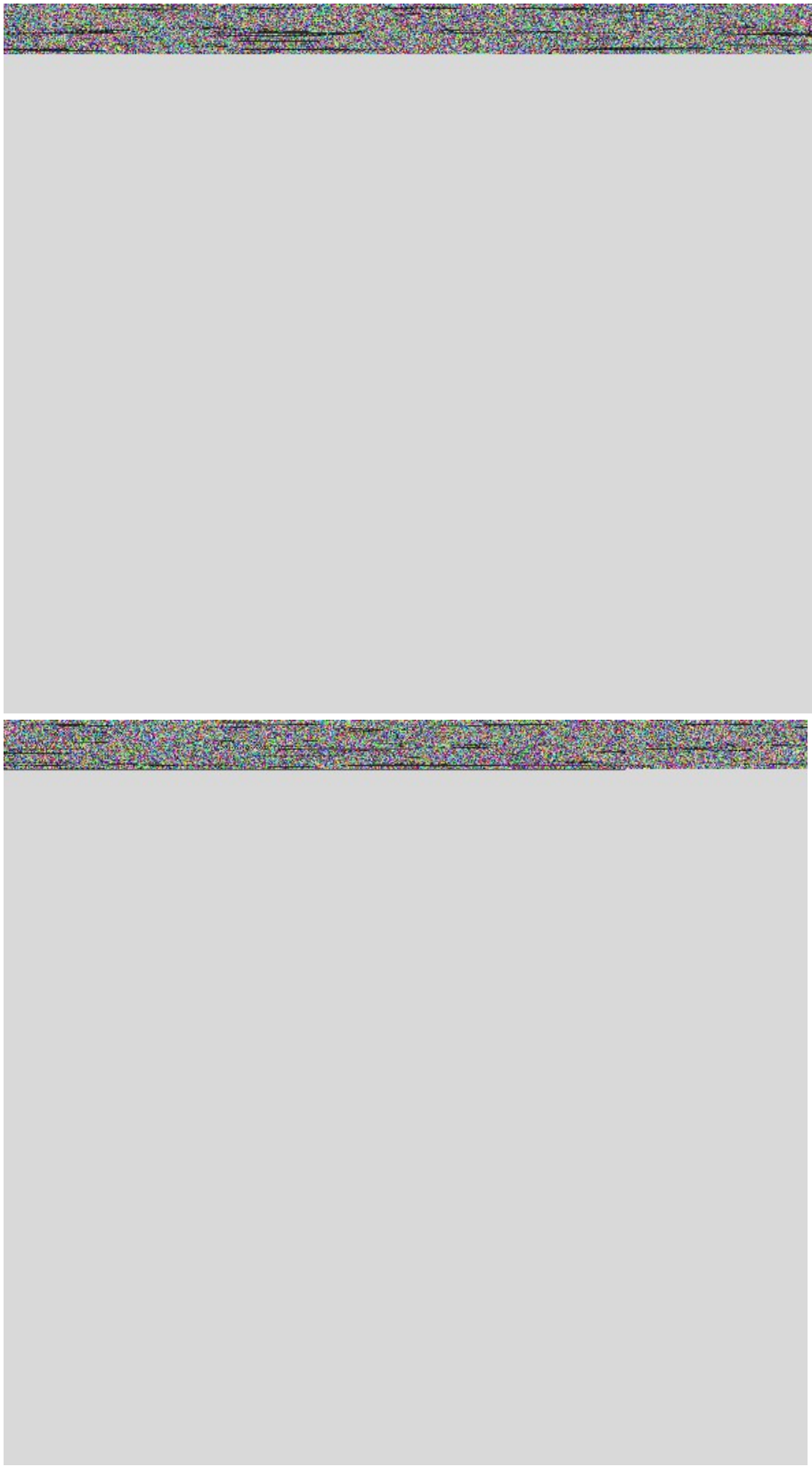

Figure 51. The post-indent AFM scans (3D) of the residual indents of crystals for the (2′*S*)-^{i}Pr **3a** and (2′*S*)-^{t}Bu **4a** crystals. The black arrows show cracks. The scan size of all the AFM images is 20 μm x 20 μm.

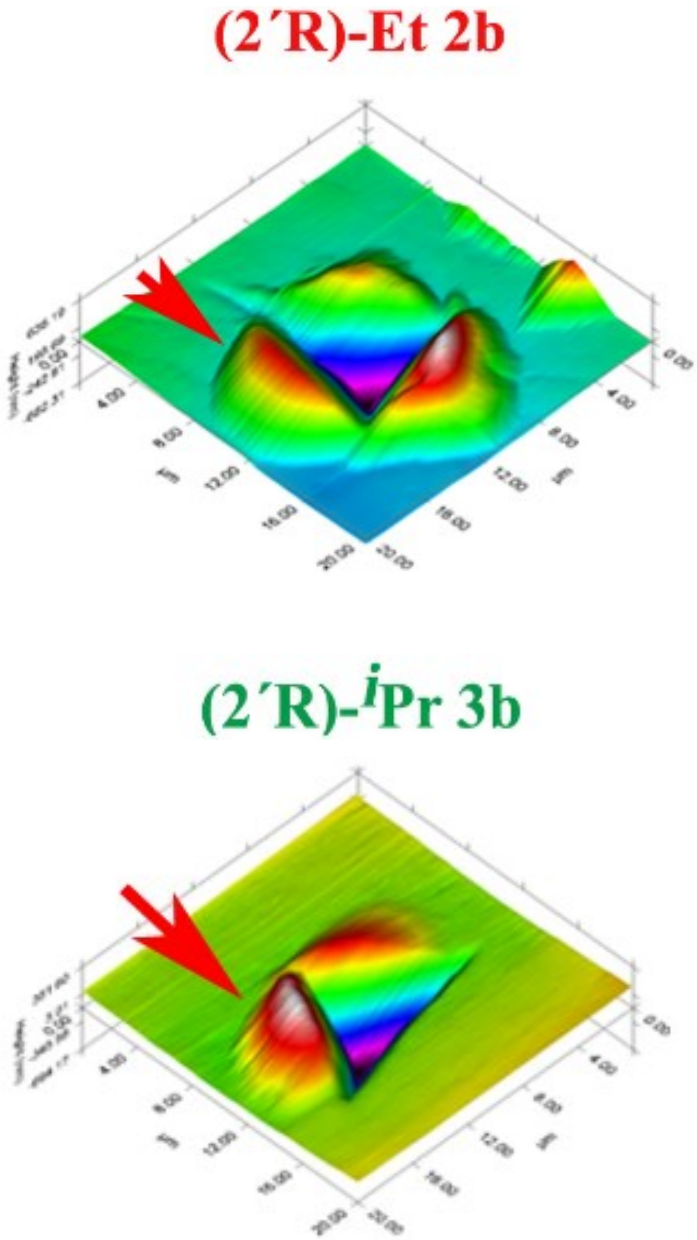

Figure 52. The post-indent AFM scans (3D) of the residual indents of crystals for the (2′*R*)-Me **1b** and (2′*R*)-Et **2b** crystals. The red arrows show pile-up. The scan size of all the AFM images is 20 µm x 20 µm.

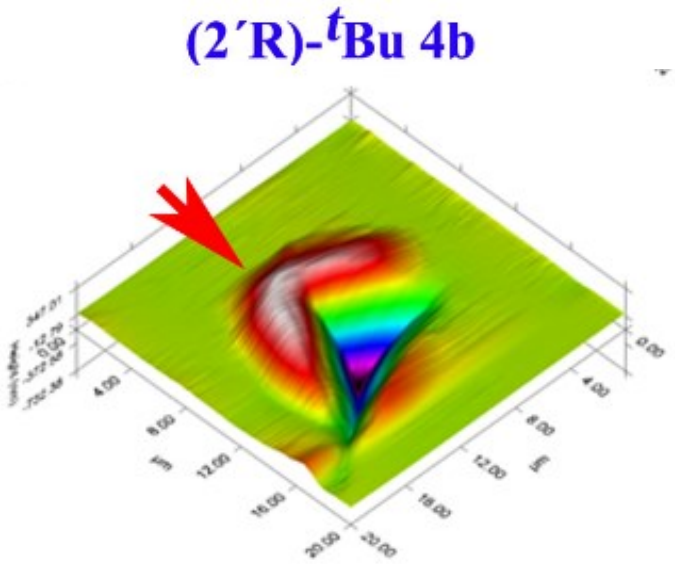

Figure 53. The post-indent AFM scans (3D) of the residual indents of crystals for the (2´*R*)-^{t}Bu **4b** crystals. The red arrow shows pile-up. The scan size of all the AFM images is 20 µm x 20 µm.

Table 1. Hardness and Modulus for **1a** and **1b**.

Sample	Hardness (GPa)	Modulus (GPa)
(2´*S*)-Me **1a**	**0.293±0.037**	**9.10±0.51**
(2´*R*)-Me **1b**	**Unable to measure (Very thin flakes)**	**Unable to measure (Very thin flakes)**

References

1 T. Hashimoto, Y. Naganawa, T. Kano, K., Maruoka, *Chem. Commun*. 2007, 5143-5145.

2 Y. Zhang, Y. Yao, L. He, Y.Liu, L., Shi, *Adv. Synth. Catal*. 2017, **359**, 2754-2761.

3 X. Luo, G. Chen, L. He, X., Huang, *J. Org. Chem*. 2016, **81**, 2943-2949.

4 Z. Yu, Y. Li, J. Shi, B. Ma, L. Liu, J., Zhang *Angew. Chem. Int. Ed*. 2016, **55**, 14807-14811.